PLOS PATHOGENS

Assessing bnAb potency in the context of HIV-1 envelope conformational plasticity

Caio Foulkes[1☯], Nikolas Friedrich[1☯], Branislav Ivan[1¤a‡], Emanuel Stiegeler[1‡], Carsten Magnus[1¤b], Daniel Schmidt[1], Umut Karakus[1], Jacqueline Weber[1], Huldrych F. Günthard[1,2], Chloé Pasin[1,2], Peter Rusert[1], Alexandra Trkola[1]*

1 Institute of Medical Virology, University of Zurich (UZH), Zurich, Switzerland, 2 Department of Infectious Diseases and Hospital Epidemiology, University Hospital Zurich (USZ), University of Zurich (UZH), Zurich, Switzerland
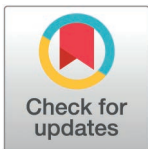
☯ These authors contributed equally to this work.
‡ These authors also contributed equally to this work.
¤a Current address: Laboratory Medicine, Division of Clinical Chemistry, University Hospital Basel, Basel, Switzerland
¤b Current address: Roche Information Solutions, F. Hoffmann-La Roche AG, Basel, Switzerland
* trkola.alexandra@virology.uzh.ch

Abstract

For use in prevention and treatment, HIV-1 broadly neutralizing antibodies (bnAbs) have to overcome Env conformational heterogeneity of viral quasispecies and neutralize with constant high potency. Comparative analysis of neutralization data from the CATNAP database revealed a nuanced relationship between bnAb activity and Env conformational flexibility, with substantial epitope-specific variation of bnAb potency ranging from increased to decreased activity against open, neutralization-sensitive Env. To systematically investigate the impact of variability in Env conformation on bnAb potency we screened 126 JR-CSF point mutants for generalized neutralization sensitivity to weakly neutralizing antibodies (weak-nAbs) depending on trimer opening and plasma from people with chronic HIV-1 infection. 23 mutations resulted in a highly neutralization sensitive phenotype, which was associated with de-stabilization of the closed, prefusion conformation. Including 19 of these mutants into a Sensitivity Env mutant panel (SENSE-19), we classified bnAbs according to potency variations in response to trimer opening. To verify that these sensitivity patterns are independent of the in vitro assay system, replication-competent SENSE-19 mutant viruses were tested on primary CD4 T cells. While loss of potency on SENSE-19 was registered for bnAbs from several classes recognizing quaternary epitopes on pre-triggered Env, structural destabilization benefitted MPER bnAbs and other inhibitors known to have post-CD4 attachment neutralization activity. Importantly, for a subset of CD4bs bnAbs, and the interface bnAb PGT151, particularly low potency variation was noted, suggesting that Env conformational tolerance can be achieved but is not the rule. In summary, SENSE-19 screens revealed distinct tolerance levels to Env conformational intermediates between bnAbs that provide mechanistic insights in their function and broaden current neutralization breadth assessments.

Author summary

High breadth and potency in neutralizing genetically divergent strains of HIV-1 is a prerequisite for the use of HIV-1 broadly neutralizing antibodies (bnAbs) in vaccines, prevention and therapy. Neutralizing antibodies (nAbs) target the HIV-1 envelope glycoprotein (Env) trimer, which conformationally shields most neutralization sensitive regions of Env in its closed, unliganded state. Due to its inherent flexibility the Env trimer can adopt alternate conformations which impact the potency and breadth of nAbs. Here we present a mutant Env virus panel that can be used to assess the dependence of neutralizing antibodies on open or closed Env conformations, allowing the identification of bnAbs tolerant to Env conformational changes.

Introduction

Broadly neutralizing antibodies (bnAbs) are central to ongoing efforts to develop effective HIV-1 vaccines and therapeutics [1–3]. The principal capacity of bnAbs to counter the extraordinary diversity of HIV-1 strains is compelling, but bnAb breadth and potency need to be at highest possible level to register in in vivo efficacy as recently demonstrated in animal models [4,5] and by the Antibody Mediated Prevention (AMP) trial in humans [6].

Activity of neutralizing antibodies (nAbs), including bnAbs, is steered by the accessibility of their epitopes on the intact HIV-1 envelope protein (Env) trimer [4,5,7–13]. Changes in amino acid composition or glycosylation conferring resistance to a distinct nAb class may often have no consequence on other nAb types. Generalized effects on neutralization sensitivity affecting multiple nAb epitopes are, however, observed when modulations in Env conformational stability occur [14–17]. Conformational flexibility and plasticity are inherent features of the HIV-1 Env trimer required for its function in entry [9,17–20]. This property, reflected also in its genetic variability, provides means for evasion by mutating and conformational masking of neutralization sensitive epitopes [11,21–24]. During host cell entry the trimeric Env protein undergoes a series of conformational changes which are driven by sequential engagement of the primary receptor CD4 and a co-receptor, ultimately leading to fusion of the virus and host cell membranes. The structural changes in the Env trimer upon CD4 binding are characterized by the transition from a "closed" to downstream "open" conformations exposing the co-receptor binding site as well as additional neutralization sensitive epitopes [8,9,18,20,25]. The activity of individual nAbs against Env structural intermediates has not been systematically investigated and thus remains not fully understood. Furthermore, the inherent Env conformational heterogeneity of viral quasispecies in vivo, comprising closed and incompletely closed Env conformations, may greatly impact neutralization efficacy [12,26–31].

Typically, gross increases in Env neutralization sensitivity coincide with high Env conformational flexibility [14,15,17,25]. This can result in altered entry kinetics as shown for macrophage-tropic HIV-1 strains that adapted to low CD4-receptor levels [15,16,32–35]. Trimer opening provides access to multiple nAb epitopes and corresponding viruses are classified as Tier 1 strains in the neutralization sensitivity ranking of viral strains [36]. The Tier-system [36], a relative measure for the sensitivity of individual HIV-1 strains to Ab-mediated neutralization, is based on the resistance of HIV-1 strains to polyclonal Abs in plasma from people with HIV-1 (PWH) derived in chronic HIV-1 infection. Lab-adapted and highly sensitive primary HIV-1 strains are categorized as Tier 1A strains. Tier 1B, Tier 2 and

Tier 3 strains are increasingly resistant to plasma neutralization, with Tier 2 comprising the majority of strains circulating worldwide [36].

The two main quality measures of bnAbs are their neutralization breadth against genetically divergent HIV-1 strains including different subtypes and the potency at which these strains are neutralized. In an effort to define bnAbs with the highest breadth and potency, their neutralization activity against >100, in some cases close to 200 virus strains from different subtypes is assessed in Env pseudovirus neutralization assays [37–39]. Algorithms for predicting bnAb epitopes and delineating neutralizing reactivity in polyclonal PWH plasma have been developed based on the wealth of information available from detailed analysis of bnAb neutralizing activity against these divergent strains [40,41]. While the careful analysis of lead bnAbs on such large virus panels is highly informative, initial screening of patient plasmas and monoclonal antibodies (mAbs) must rely on smaller virus panels to enable higher sample throughput in determining neutralization breadth [42,43]. Here we report on an alternative approach to identify and characterize lead bnAbs employing single site Env mutants with reduced conformational stability that allow discriminating bnAbs from weak-nAbs. Moreover, systematic evaluation of the tolerance of bnAbs to trimer opening provides a measure to classify bnAbs according to their breadth and potency.

Results

Assessing bnAb potency in the context of HIV-1 Env conformational plasticity

bnAbs, per definition, inhibit genetically divergent virus strains and retain high activity against Tier-2 viruses known to largely maintain a closed prefusion Env conformation [7,17,20,44,45]. While effects of modulating Env stability on neutralization activity have been described for some bnAbs [15,16,46,47], a refined understanding of how Env conformational plasticity affects neutralization efficacy across bnAb types remains important. To compare bnAb activity over the full spectrum of highly flexible to less flexible Envs, we used Tier-based neutralization data available in the CATNAP database (http://hiv.lanl.gov/catnap) [48] (Fig 1). We selected 21 prototypic bnAbs covering the five major bnAb epitopes for this analysis (CD4-binding site (CD4bs) bnAbs VRC01, NIH45-46, PGV04, 3BNC117, N6, N49P7 and VRC07-523; V2-glycan bnAbs PG9, PG16, PGDM1400, and PGT145; the gp120-gp41 interface bnAb PGT151; the V3-glycan bnAbs PGT121, PGT 128, PGT130, PGT135, BG18 and 2G12; and bnAbs against the membrane proximal external region (MPER) in gp41: 4E10, 10E8, and 2F5). Several weak-nAbs that represent Ab specificities prevalent at high titers in HIV-1 infection were chosen for comparison [49,50]. These included nAbs to the variable region 3 (V3-crown: 447-52D and 1–79), the CD4-induced epitope (CD4i: 17b) and agents directed to the CD4bs (nAbs 1F7 and b12, and the CD4 receptor analogue CD4-IgG2). Access to these epitopes requires either partial or full, spontaneous or receptor-induced conformational opening of the trimeric Env complex [9,13,51]. Geometric mean IC50 values stratified by neutralization Tier showed the expected pattern with weak-nAb activity being almost exclusively restricted to Tier 1 strains (Fig 1). This is in line with the more tightly closed Env prefusion conformation of higher tiered Envs disfavoring antibody attack by increased conformational shielding and/or altering entry kinetics [14–17,25,34].

Interestingly, side-by-side comparison of the inhibitory activity of different bnAb classes against tiered viruses revealed, that bnAbs also benefit from some degree of Env trimer opening. A gradual decrease in potency with increase in Tier-level was evident for most bnAbs (Fig 1A). CD4bs and MPER directed bnAbs inhibited Tier 1A viruses most potently. V2-glycan bnAbs and the interface directed bnAb PGT151 showed a multi-phase activity
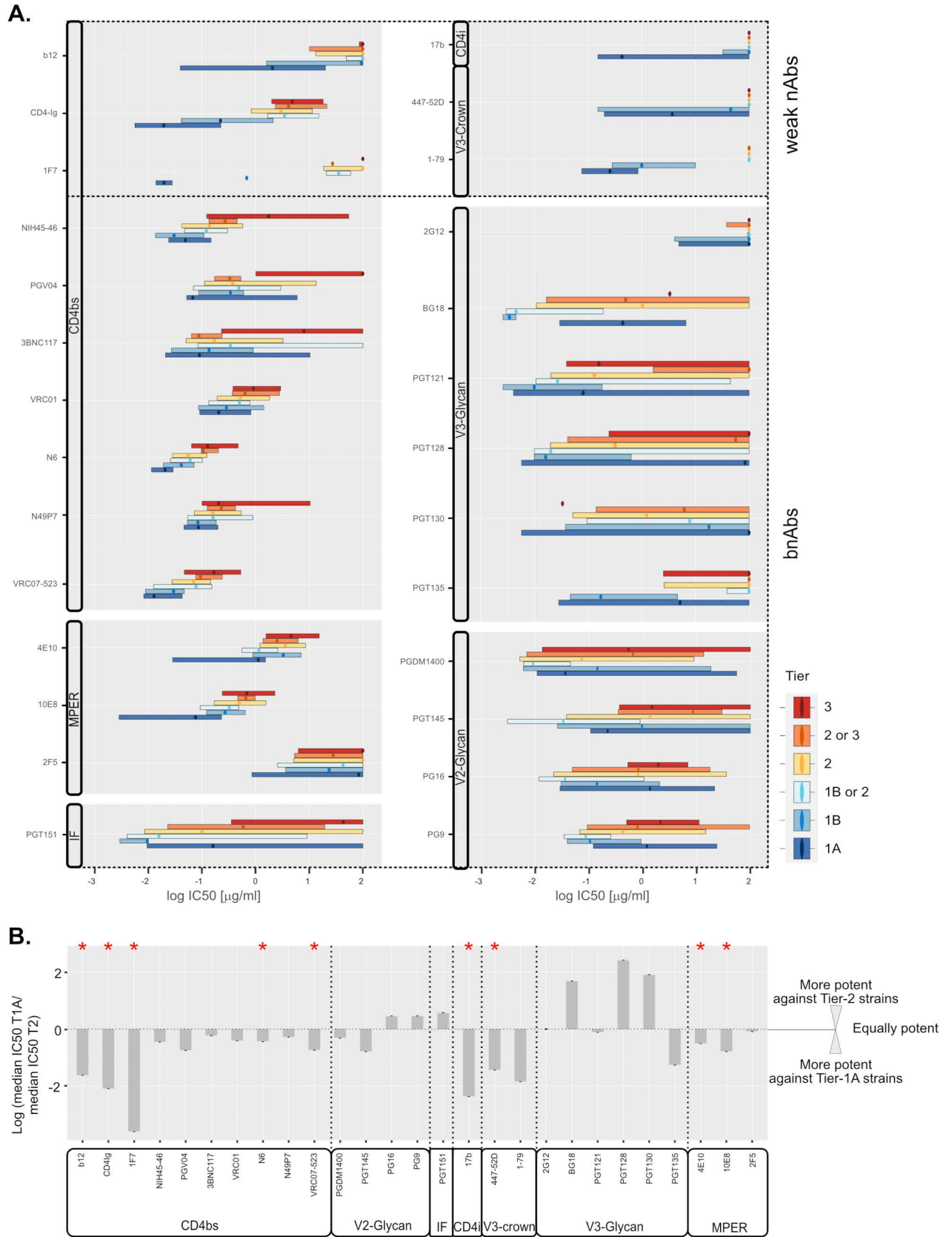
Fig 1. **Ab-specific variations in neutralization potency against HIV-1 strains assigned to different neutralization tiers.** All IC50 data available from the Los Alamos National Laboratory database (http://hiv.lanl.gov/catnap; as of October 2024) was downloaded for the antibodies listed

(grouped by epitope as indicated) against all HIV-1 strains that had been attributed to a neutralization tier (tier 1A: most sensitive; tier 3: most resistant, see S1 Table for the neutralization data available per Ab and tier). **A.** Distribution of IC50 values for each antibody and for HIV-1 strains of different tiers (dots: median, boxplot: values within the interquartile range; whiskers indicating minimum and maximum values were omitted for clarity). **B.** Summary of differences between median potencies of Abs against Tier 1A and Tier 2 strains. Significant differences (p < 0.05, Mann-Whitney test) are indicated by a red star.

https://doi.org/10.1371/journal.ppat.1012825.g001

pattern with Tier 1A and Tier 3 strains recording the lowest neutralization sensitivity and peak potency against Tier 1B or Tier 1B/2 classified strains. Patterns of V3-glycan bnAbs were diverse, but most of the tested V3-glycan bnAbs showed highest potency against either Tier 1A or Tier 1B viruses. While differences in median IC50 between Tier 2 and Tier 1A for bnAbs were in most cases within 0.5–1 orders of magnitude (Fig 1B), the differences for weak-nAbs remained the most pronounced (>1.5 orders of magnitude) leading in several cases to a switch from no activity to potent neutralization which is prototypical for mAbs against CD4i and V3-crown epitopes [11,16,52].

Harnessing perturbations in Env conformation to classify bnAb activity

The higher activity of most bnAbs against lower-tier viruses suggests a general effect of relaxing Env conformational stability on bnAb potency. We therefore hypothesized, that patterns of neutralizing activity based on Env stability could be used to classify nAbs. To explore this in a controlled setting, we utilized a panel of single-site gp120 mutants of the subtype B Tier 2 strain JR-CSF covering 125 of the 503 gp120 amino acid positions [38,53,54] (Figs 2 and S1). To select mutants with a generally enhanced neutralization sensitivity, JR-CSF mutant pseudoviruses were screened against plasma from people with chronic, untreated HIV-1 infection (N = 18; S2 Table), the CD4 receptor analogue CD4-IgG2 and a range of weak-nAbs (CD4bs: b6 and b12, V3-crown: 1–79, 447-52D).

Consistent with the limited cross-neutralizing activity observed in HIV-1 infection, JR-CSF wild-type (wt) was neutralized by only a subset of plasmas (11/18) (S1A and S1B Fig). While the majority of gp120 mutations did not lead to a relevant change in neutralization sensitivity, 23 mutants displayed a high (>10-fold above wt) and 7 mutants a moderate (4–10 fold above wt) median increase against plasma (Fig 2A). Notably, these mutants also recorded high and modest neutralization sensitivity against plasma samples, that were inactive against JR-CSF wt (S1A and S1B Fig) and across plasmas from individuals with different subtype of infection (S1C Fig), demonstrating a general release of conformational shielding in these 30 mutants. This was supported by the inhibition data with weak-nAbs. Only few mAb-mutant combinations deviated from this overall pattern of increased sensitivity, suggesting that in these cases the mutation directly affected the mAb epitope. Collectively, the 30 neutralization sensitive mutants recorded with a >10-fold enhanced sensitivity to at least one V3-crown mAb (1–79, 447-52D) and one CD4bs directed inhibitor (b6, b12 or CD4IgG2) (Fig 2B and S3 Table).

Known resistance inducing mutations were confirmed for some bnAbs. However, in contrast to weak-nAbs, bnAbs showed no or comparatively moderate increases in neutralizing potency across the mutant panel regardless of their specificity, with only a few bnAb-mutant combinations reaching a 10-fold increase, most of which fell within the 30 defined mutants with generally enhanced neutralization sensitivity (2G12: 2/2; PGT135: 1/1; 2F5: 9/10; 4E10: 9/9; 10E8: 3/5) (Fig 3A). Notably, the most consistent increase in neutralizing activity against these mutants was observed for MPER bnAbs known to exert their neutralizing activity primarily after CD4 binding, when concomitant Env trimer opening increases MPER exposure [10,33,55]. Modest potency gains were also observed for 2G12 and for PGT135 which, similar to MPER bnAbs, has been found to harbor post-attachment neutralization activity [10]. The CD4bs bnAbs VRC01, VRC07-523, N6 and N49P7 recorded the strongest gain in potency

A.

B.
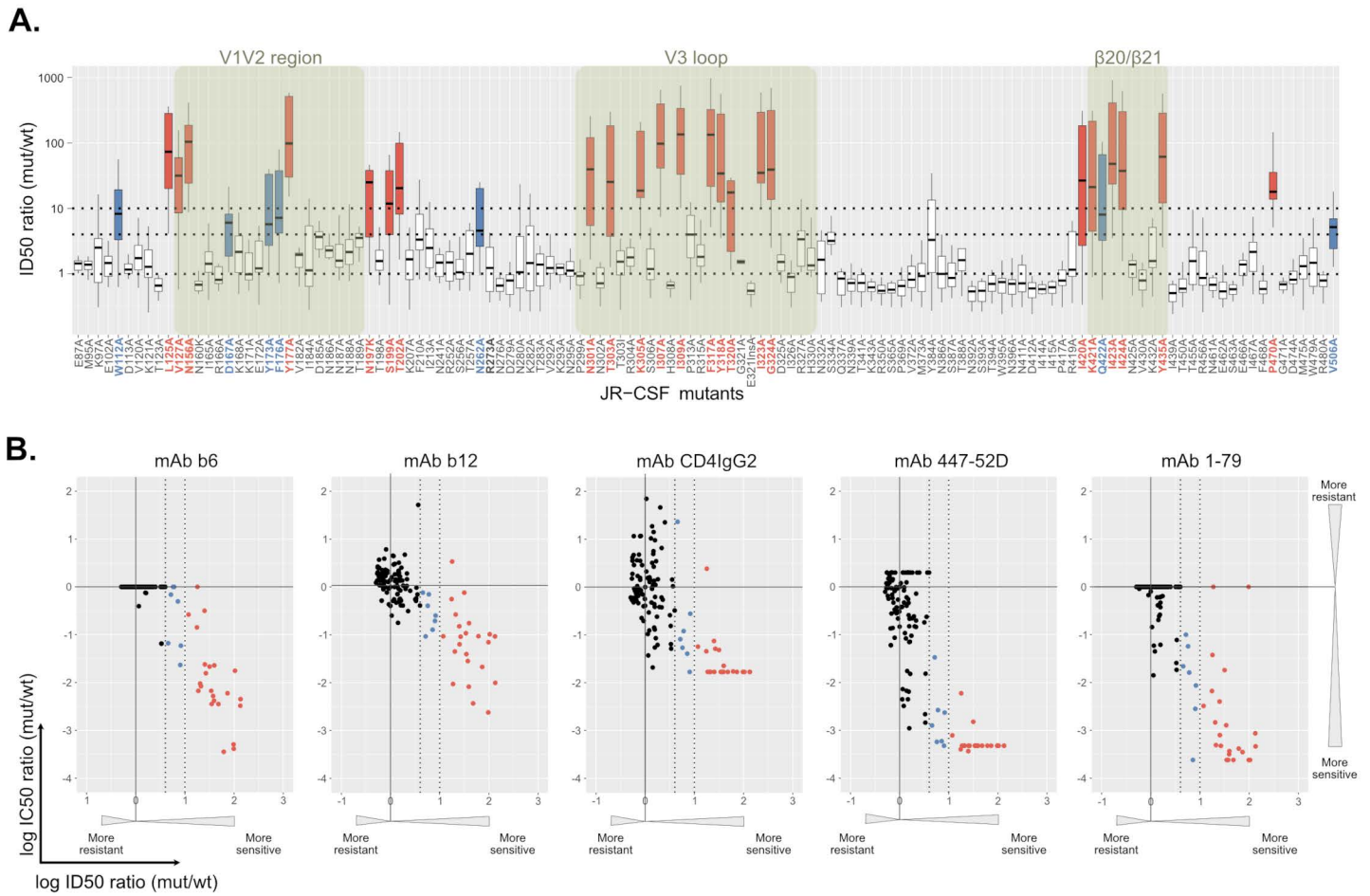
Fig 2. Characterizing the generalized neutralization sensitivity of JR-CSF envelope point mutants. The neutralization sensitivity of 126 JR-CSF envelope (Env) mutants was determined in a TZM-bl based pseudovirus inhibition assay. **A.** Each mutant virus was titrated with eleven plasma samples from HIV-1 chronically infected individuals (nine subtype B infected, two infected with non-B subtypes). All eleven plasmas neutralized JR-CSF wild-type virus at an inhibitory dilution (ID50) > 100, the minimal dilution probed. The distribution of ID50 ratios (mutant/wt) is shown for each mutant (center line: median; box limits extend from the 25th to 75th percentiles; whiskers indicate minimum and maximum values). A dotted line at ID50 ratio (mutant/wt) = 1 indicates equal neutralization sensitivity of the mutant Env compared to the wildtype reference. Thresholds used for categorizing mutants into highly (ID50 ratio (mutant/wt) >10; colored red) and moderately (10 > ID50 ratio (mutant/wt) >4; colored blue) sensitive phenotypes are indicated by dotted lines. **B.** IC50 values determined for each mutant against CD4 binding site (CD4-IgG2 and mAbs b6 and b12) and V3-crown (mAbs 1–79 and 447-52D) directed inhibitors were compared with median plasma ID50s as determined in A. Colorcode as in A. Titrations of each plasma and antibody on all viruses was done once, except for the JR-CSF wt reference for which plasma ID50s and nAb IC50s were derived by fitting a curve to pooled datapoints from n ≥4 titrations.

upon mutation of the N197 glycosylation sequon in line with the reported shielding of the CD4bs by this glycan [56,57]. Otherwise, these CD4bs bnAbs showed no increase in neutralization potency >10-fold across the entire panel. Equally no gain in potency was observed for the V2-apex bnAb PGT145 and the V3-glycan bnAbs PGT121, PGT128, and PGT130.

Distinct, general patterns of activity of weak-nAbs, bnAbs, and patient plasma across the mutant panel were revealed by Spearman correlation analysis (Fig 3B). Antibody reactivity patterns fell into four categories defined by hierarchical clustering: cluster I characterized by strong positive correlation amongst plasma, weak-nAbs and bnAb PGT135, cluster II comprising MPER bnAbs, 2G12 and N6 with low but consistent positive correlation to cluster I, cluster III with V3-glycan bnAbs (PGT121, PGT128 and PGT130) as well as V2-glycan bnAb PGT145 showing negative correlations to cluster I and cluster IV containing CD4bs bnAbs
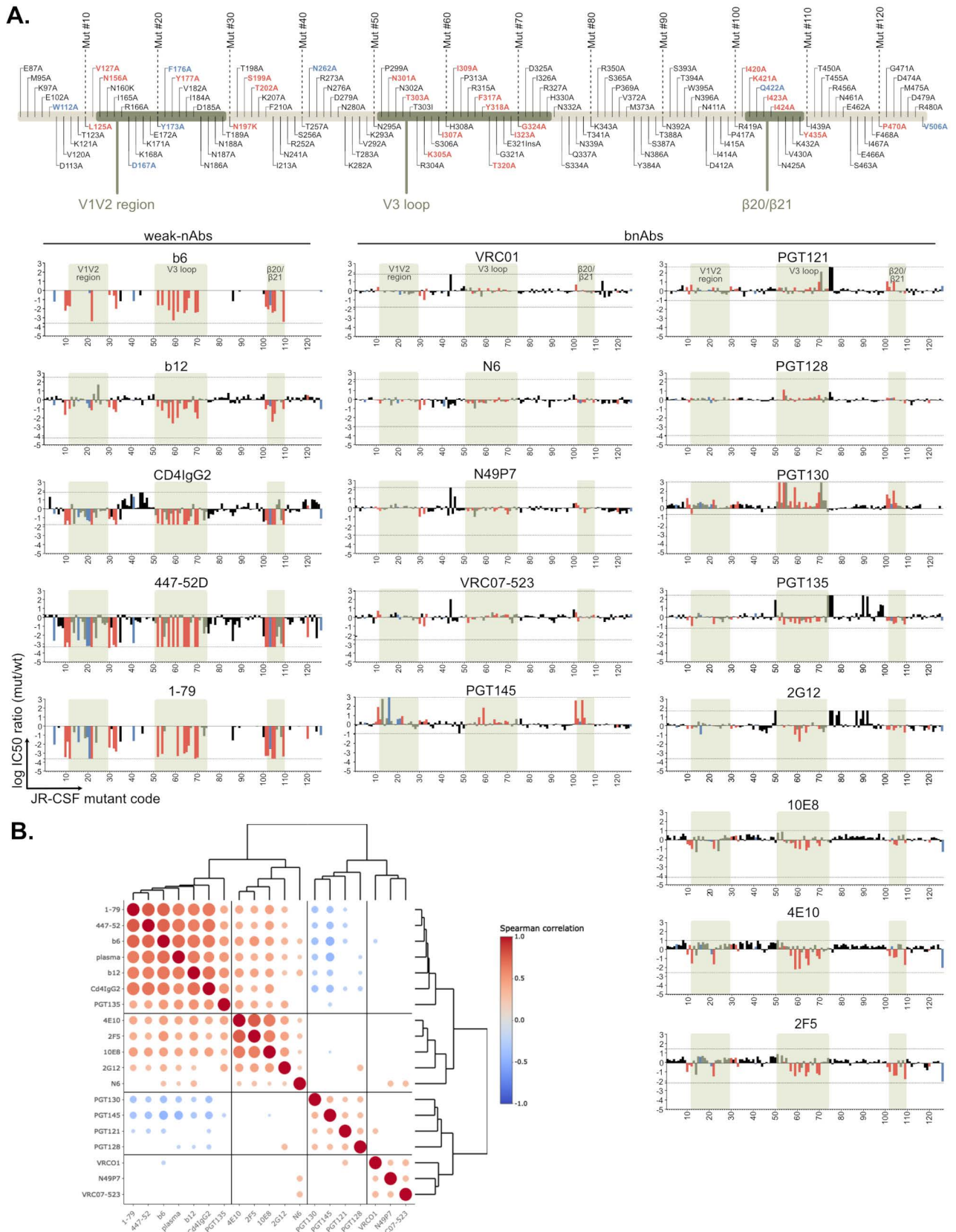
Fig 3. HIV-1 Env generalized neutralization sensitivity impacts differentially on the potency of broadly neutralizing antibodies (bnAbs). The whole JR-CSF Env mutant panel was tested for neutralization sensitivity against bnAbs targeting four major epitopes (CD4bs: VRC01, VRC07-523,

N6 and N49P7; V3-glycan: PGT121, PGT128, PGT130, PGT135; 2G12; V2-glycan: PGT145; MPER: 2F5, 4E10, 10E8). **A.** Graphs show the log IC50 ratio (mutant/wt) for each Env mutant. IC50 ratios corresponding to minimal and maximal concentrations of inhibitors probed are indicated with lines. Weak-nAb data from Fig 2B is shown for comparison. The order of Env mutants and shaded regions of interest are indicated on top. Titrations of most antibodies on all viruses was done once (n = 1), except for the JR-CSF wt reference (n ≥ 4). mAbs PGT128, PGT145, 10E8 and 2G12 were titrated twice (n = 2) on all mutants. **B.** Spearman correlation matrix and hierarchical clustering of neutralization fingerprints based on IC50 data in A and Fig 2. For correlation with PWH plasma the median reciprocal ID50 ratio (mut/wt) over 11 JR-CSF wt neutralizing plasma (Fig 2A) was used. All significant correlations (p-value ≤ 0.05) are indicated with a circle with bigger circles indicating stronger support (lower p-values).

https://doi.org/10.1371/journal.ppat.1012825.g003

VRC01, VRC07-523 and N49P7 for which no consistent correlations with other clusters were detected.

The similarity of MPER bnAbs and PGT135 with plasma and weak-nAb inhibition patterns underscores that the activity of these Abs benefits from structural destabilization of the trimer. PGT135 and 2G12 target overlapping epitopes including glycans at positions N295, N332 and N386 [58,59] suggesting that their simultaneous engagement by these two Abs is to some extent facilitated by enhanced conformational flexibility of the trimer. Conversely, a decreased activity of PGT145 against less stable trimers is expected as its quaternary V2-glycan epitope at the trimer apex depends on close vicinity of the gp120 protomers [60]. The data further suggested that PGT130, which like PGT121 and PGT128 binds the GDIR motif at the V3-base but differs in the dependency on glycans located in V1V2 (N137, N156) and V3 (N301, N332) [61,62], may also benefit from a more restrained closed conformation.

Collectively, the reactivity pattern highlighted qualitative differences of bnAbs, and suggests that the most potent and broad CD4bs bnAbs including VRC01, VRC07-523 and N49P7 show a comparatively high tolerance towards perturbation in Env conformational stability. Notably, however, we observed a modest increase in potency related to trimer opening for CD4bs bnAb N6, despite its already high potency.

Generalized increases in neutralization sensitivity link with de-stabilization of the closed prefusion Env conformation

To explore common antigenic features associated with a generalized neutralization sensitivity we probed five moderately and 22 highly neutralization sensitive Env mutants in a cell-based binding assay. Cell-expressed Envs were triggered by increasing doses of soluble CD4 (sCD4) and gradual opening of the trimer measured by the binding intensity of the prototypic CD4i mAb 17b that depends on trimer opening to access its epitope [17,63–67] (Fig 4A). JR-CSF wt and the N332A mutant, which showed no increased neutralization sensitivity, were added for comparison. N332A and wt Env failed to bind 17b in absence of sCD4 trigger while the majority of the sensitive mutants (20/27) bound 17b (Figs 4B, S2A and S2B). Neutralization sensitive mutants (7/27) that did not bind 17b in absence of sCD4 included mutants in residues 420–424 and 435 which are known to impact on 17b binding to monomeric gp120 [65]. In none of these cases 17b binding was however completely abolished since all neutralization sensitive mutants displayed a notable increase in 17b binding upon CD4 triggering. sCD4 dose escalation revealed that 24 out of 27 neutralization-sensitive mutants had a markedly increased propensity to adopt an open conformation, consistent with a decreased stability of the closed pre-fusion conformation in these mutants (Figs 4B and S2A and S2B). For the remaining three mutants (W112A, Y173A, and P470A) a more moderate effect was noted.

To link 17b exposure to neutralization sensitivity we measured the neutralization potency of 17b against 19 Env mutants with high general sensitivity alongside controls (S2C Fig). Excluding mutants known to directly affect the 17b epitope (I420A, I423A, I424A, Y435A)
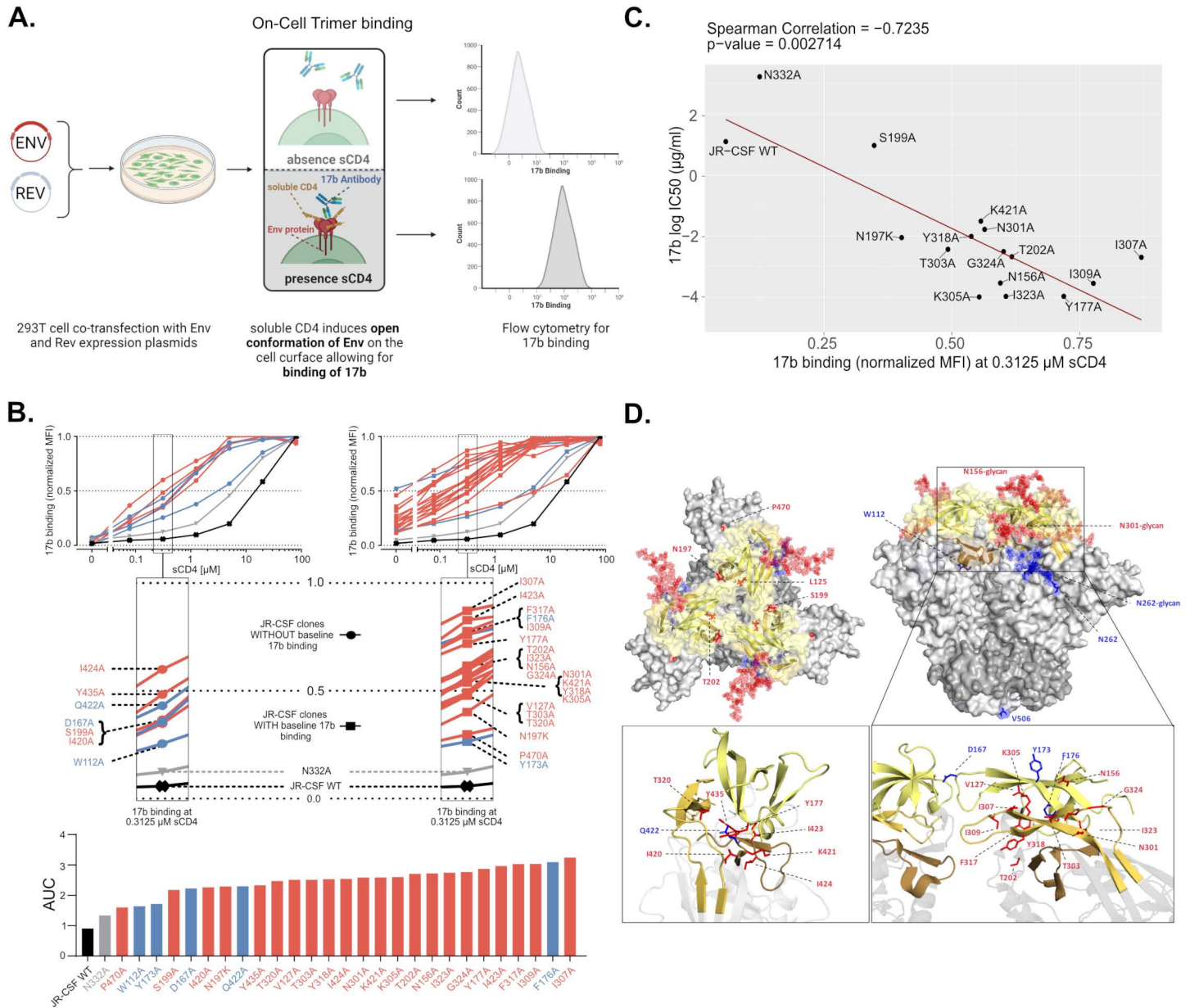
Fig 4. Characterizing the exposure of the co-receptor binding site by neutralization sensitive Env mutants. A. Schematic illustrating the experimental sCD4-induced opening of cell surface expressed Env leading to exposure of the co-receptor binding site. For detection by flow-cytometry mAb 17b was used as a co-receptor mimic. **B.** Top panel: Opening of cell surface expressed Envs by increasing concentrations of sCD4 was monitored by staining with mAb 17b. Env mutants were divided into two groups showing enhanced 17b binding in absence of sCD4 (right) or not (left) compared to JR-CSF wt Env. The N332A mutant served as additional control. All titrations were performed once. Color code of mutant sensitivity as in Fig 2. Middle panel: magnification of top panel data indicating data points for 17b staining of individual Env mutants. Bottom panel: The bar graph depicts area under the curve values derived from the normalized MFI curves of the top panel graphs. **C.** Spearman correlation between 17b neutralization sensitivity of JR-CSF wildtype and mutant viruses and 17b binding according to B. Mutations directly affecting 17b binding [65] were not included (see also S2C Fig). **D.** Alanine-substitutions leading to moderate (blue) or high (red) generalized neutralization sensitivity of the JR-CSF Env were mapped onto the trimeric closed prefusion structure of the closely related JR-FL Env ectodomain (PDB: 5FYK; V1V2: yellow, V3: orange, β20-β21: brown, gp120: light grey, gp41: dark grey). Glycans on neutralization sensitive positions N156, N262 and N301 are depicted. The N197 glycan is not shown as JR-FL naturally lacks this PNGS.

https://doi.org/10.1371/journal.ppat.1012825.g004

[65,68], the remaining mutants all showed high 17b sensitivity. 17b neutralizing activity and binding were tightly correlated confirming a propensity for trimer opening as a common trait of generalized neutralization sensitivity (Figs 4C and S2C).

Mapping of the 30 JR-CSF Env mutations that confer generalized sensitivity on the crystal structure of the trimeric Env ectodomain from the closely related JR-FL strain (Fig 4D) highlights their positioning in domains relevant for conformational stability of the trimer [15,16,46]. The majority of mutations (26/30) were concentrated in and around V1V2, V3 and β20-β21 strands of the bridging sheet. The remaining four were mapped to C1 (W112A), C2 (N262A) and C5 (P470A and V506A). For three out of the 30 amino acids interactions mediated by the side chains were identified in the structure (D167: interprotomer salt bridges to T128 and R192; K305: intraprotomer salt bridge to E172; Y435: intraprotomer hydrogen-bonds to Y318 and T319), which are likely disrupted by mutation to alanine, providing an explanation for the observed destabilization of the closed conformation (S3A Fig). Glycans in gp120 contribute both to shielding and trimer stability [69]. JR-CSF wt contains 23 potential N-glycosylation sites (PNGS) within gp120. 17 of these PNGS were mutated in the full JR-CSF mutant panel (N = 126; Figs 2 and S1) and four of them (N156A, N197A, N262A and N301A) were associated with a generalized-sensitivity phenotype. As these residues are known to be important for Env stability [60,70,71], the gain in sensitivity upon loss of the glycosylation site may stem from both, a regained access to an epitope covered by this glycan or an increased propensity for trimer opening. Indeed, N197 has been shown to be critical for trimer integrity and neutralization resistance in several HIV-1 strains [34,72–74], as the associated glycan is positioned to protect both V3 and the CD4bs [56,57]. We also observed a dual role for the N301 PNGS in shielding and trimer stability. The decreased Env stability and increased neutralization sensitivity of N301A and T303A mutants was partially rescued in a T303I mutant, suggesting that the amino acid type in position 303 is also important (Figs 2 and 3 and S2D).

HIV-1 relies on the closed Env prefusion conformation to protect itself against antibody mediated neutralization [9,11,15,16]. Analysing group M Env sequences in the Los Alamos National Laboratory database (N = 6084, super-filtered web alignment (2021), including group M and CRFs, http://www.lanl.com/), we observed different degrees of conservation for the 30 positions associated with generalised sensitivity in JR-CSF Env. Notably, 19 of the positions were recorded with >90% preservation (S3B Fig), as would be expected for positions involved in maintaining the closed state.

Focusing on mutations that confer high neutralization sensitivity in the context of JR-CSF, we next sought to investigate their role in a different Env genetic background. We chose for this the subtype A Env BG505 T332N known for its exceptional trimer stability [7,45,56,75] and generated 20 variants carrying mutations inducing high sensitivity in JR-CSF. Indeed, the majority of BG505 mutants (13/20) showed an enhanced propensity to undergo CD4-induced conformational transitions, exposing the V3-crown to a higher degree than BG505 T332N wt following sCD4 triggering (S4 Fig). However, in contrast to JR-CSF, neutralization sensitivity was increased only to CD4-IgG2 by these mutations. Other weak-nAbs and PWH plasma did not become more potent (S5 Fig). Thus, mutations at these positions can entail different degrees of conformational destabilization and neutralization sensitivity depending on the virus strain.

Neutralization fingerprinting using the JR-CSF sensitivity Env mutant panel (SENSE-19)

Considering the functional conservation of the positions associated with generally increased neutralization sensitivity we reasoned that these JR-CSF mutants may allow standardized typing of nAbs with respect to their preference and tolerance of Env structures. To ease incorporation of generally sensitive virus mutants into future nAb screens, we sought to focus on a concise collection of mutants with maximal information gain. Hierarchical clustering

of all 126 JR-CSF mutants according to their neutralization sensitivity revealed a cluster of 17 mutants with high generalized sensitivity (S6 Fig). From this group mutant F317A was excluded due to relatively low infectivity. We additionally included mutants T202A, N197K and S199A from a second cluster containing generally sensitive mutants. T202A is a naturally occurring mutation (S3B Fig). N197K and S199A mutations affect a PNGS with critical function in trimer stability and neutralization sensitivity [34,56,57,72–74]. We refer to this collection of 19 JR-CSF mutants as Sensitivity Env Mutant Panel (SENSE-19). As expected for mutations affecting trimer stability, we overserved a reduced infectivity among the SENSE-19 mutants, however the reduction was overall modest (median gp120/p24-normalized infectivity 0.47-fold compared to wt; range: 0.05- to 1.37-fold wt infectivity (S7A–S7C Fig)).

We next used SENSE-19 to establish fingerprints of larger numbers of weak-nAbs and bnAbs building on those included in the full JR-CSF mutant screen (Figs 2 and 3). SENSE-19 fingerprinting of 11 additional Abs (5 CD4bs Abs, 3 V2-glycan Abs, 1 V3-glycan Ab, 1 gp120-gp41 interface Ab and 1 CD4i Ab) showed a pattern consistent with observations made on the full panel. Weak-nAbs displayed the expected strong increase in neutralization potency while bnAbs recorded comparatively small gains in activity or resistance (Fig 5A). The fingerprints also revealed some differences in Env conformational intermediates sampled by the individual SENSE-19 mutants, as they restricted the potency of CD4bs, V2-glycan and V3-glycan bnAbs to different degree.

We further probed the performance of monovalent, broadly neutralizing DARPin (bnD) based inhibitors against SENSE-19. We included the V3-crown specific bnDs (bnD.1, bnD.2, bnD.3 and bnD.4; [51,68]) and bnDs recognizing αV3C, an alpha-helix within the V3 C--terminal strand (bnD.8 and bnD.9; [68]). All six bnDs require Env opening for binding and exhibit dominant post-attachment neutralization activity [51,68]. In agreement, the bnDs yielded notably enhanced potency across SENSE-19 (Figs 5C and S7D). Interestingly, spearman correlation analysis and hierarchical clustering of SENSE-19 neutralization fingerprints distinguished a cluster of conformation-specific inhibitors recognizing CD4-induced epitopes comprising Ab 17b as well as the bnDs tested (Fig 5B). This cluster was separate from a second cluster comprising plasma and Abs with restricted activity against closed prefusion Env and some bnAbs with dominant post-attachment activity. While most CD4bs bnAbs clustered together, other bnAb types were spread across different clusters suggesting that the bnAb type alone does not allow to predict a bnAbs conformational dependence (Fig 5B).

To differentiate nAbs and bnDs independent of potential direct interactions with residues mutated in the panel, we introduced a SENSE-19 score, defined as the median log IC50 ratio (mutant/wt) over the panel. Abs with a SENSE-19 score close to zero showed highest tolerance against changes in Env conformational stability. Particularly low variations in potency were evident for CD4bs bnAbs VRC01, VRC07-523, 1NC9, and N49P7 suggesting that CD4bs bnAbs are particularly suited to achieve high tolerance to structural changes in Env. The interface bnAb PGT151 likewise recorded with low variation in potency across the SENSE-19 panel.

Classifying Abs and bnDs according to the SENSE-19 score together with neutralization potency and breadth, we observed four categories (Fig 5C). Abs with limited potency and breadth and strong dependence on trimer opening had SENSE-19 scores <−1.5. bnAbs and bnDs that benefit from trimer opening recorded a SENSE-19 score ranging from −1.5 to −0.2. bnAbs with high tolerance to structural changes displayed SENSE-19 scores between −0.2 to 0.2 and bnAbs depending on a closed trimer conformation scored >0.2. bnAbs 3BNC117, NIH45-46, PGV04, PGDM1400 and PGT145,recorded with an overall reduced potency on SENSE-19 (score >0.2) but showed a tendency for increased neutralization potency against Tier 1A strains compared to Tier 2 strains (Fig 1B) underlining that Env conformations sampled by SENSE-19 mutants are distinct differ from those of Tier-1A viruses.
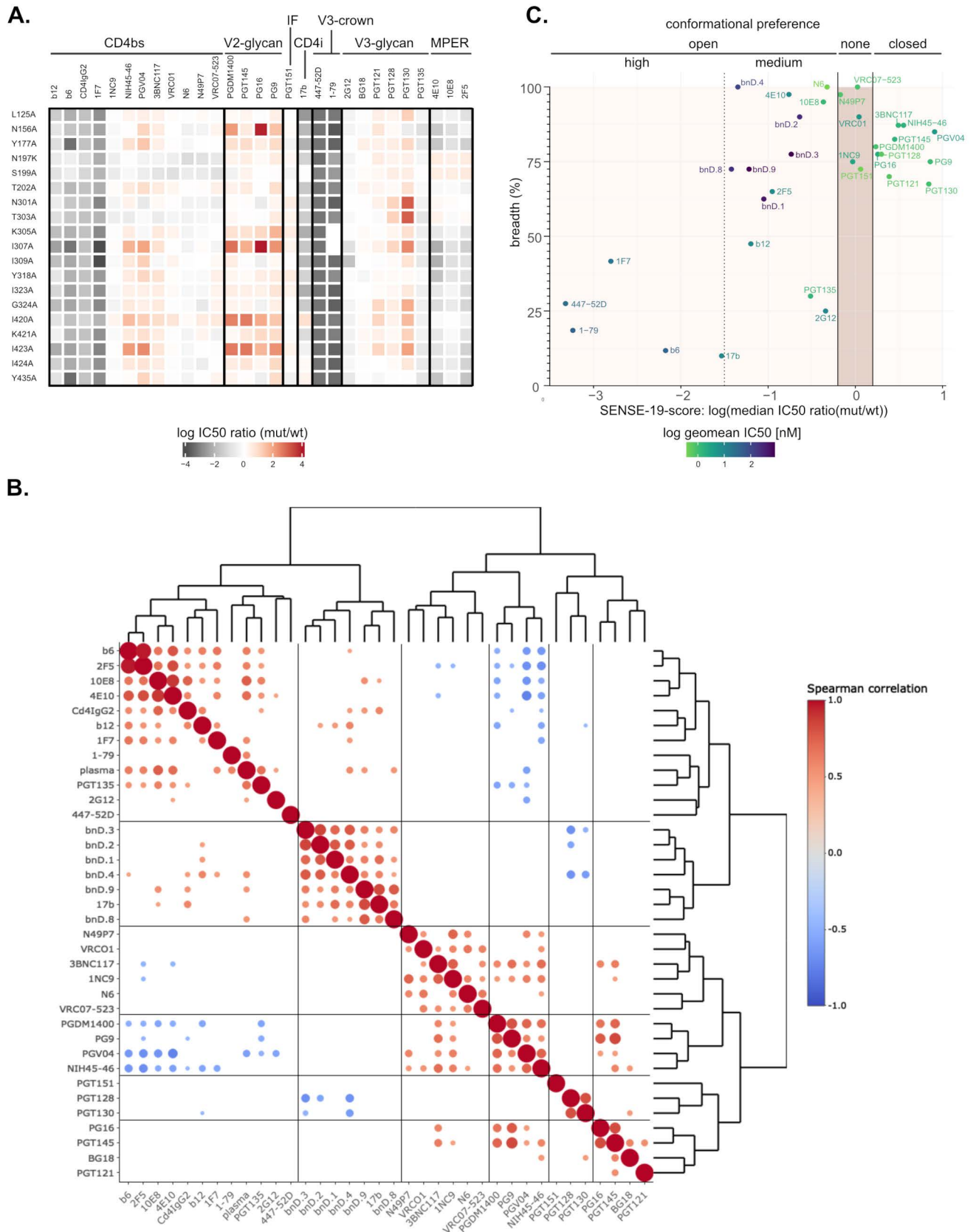
Fig 5. Neutralization fingerprinting of nAbs on a neutralization sensitive Env mutant panel (SENSE-19). Pseudovirus neutralization data on TZM-bl cells. **A.** IC50 ratios (mutant/wt) of an extended panel of nAbs were displayed as a heatmap. Abs are ordered by epitope. All titrations were

performed in one technical replicate. **B.** Spearman correlation matrix and hierarchical clustering of SENSE-19 neutralization fingerprints from Abs, bnDs and PWH plasma (median reciprocal ID50 ratio (mut/wt) over 11 JR-CSF wt neutralizing plasma (Fig 2A)). All significant correlations (p-value ≤0.05) are indicated with a circle with bigger circles indicating stronger support (lower p-values). **C.** Comparison of three Ab quality parameters: neutralization breadth, potency and SENSE-19 score. Breadth and potency were determined on a cross-subtype 40 virus panel.

https://doi.org/10.1371/journal.ppat.1012825.g005

While the SENSE-19 panel is already moderate in size, a smaller panel that yields the same information may be useful for larger screens. To probe if the number of mutants in the panel can be further reduced we conducted a random forest analysis and identified suitable panels consisting of 6 and 12 mutants, respectively (S7E Fig). The top scoring combination of 6 mutants and the top scoring combination of 12 mutants determined were then used to calculate corresponding SENSE-6 and SENSE-12 scores. Both panels classified nAbs and bnDs in a very similar manner compared to SENSE-19 (S7F Fig), confirming that use of SENSE-6 in high-throughput screens is possible. In the context of our study, we opted to continue with the larger SENSE-19 panel as this provides improved means to identify phenotypic features of distinct Env mutants and to characterize the respective Env conformational intermediates in their interaction with bnAbs. An additionally advantage of the larger SENSE-19 panel is that mutations directly affecting a bnAb epitope and leading to full resistance will not impact the readout strongly, while loss of 1 mutant out of 6 could be more critical.

Collectively, SENSE fingerprinting provides insight of bnAb tolerance to structural changes and may be used in conjunction with a conventional neutralization breadth screen to define post-attachment acting bnAbs and broadly neutralizing inhibitors.

Probing SENSE-19 mutants in the context of PBMC-based neutralization assays

An obstacle to the evaluation of neutralization activity remains the lack of standardizable, high-throughput assays to study HIV-1 inhibition in an environment similar to in vivo infection of primary CD4 T cells with replicating virus. Both the virus preparation and the variable infectivity of the target cells, peripheral blood mononuclear cells (PBMC) from random donors, are through-put limiting resources and can create a substantial assay-to-assay variability [76]. However, the use of PBMC-based neutralization in the evaluation of bnAbs has been reconsidered in recent years because the virus producer and target cells used may influence the neutralization efficacy recorded, at least for some Ab-virus combinations [76–83]. To verify whether SENSE-19 mutants record similar results in different assay systems, fingerprinting was performed in a PBMC based setup. We probed individual replication competent viruses in a conventional PBMC setup (Fig 6) and in a pooled virus library assay format similar to the approach used for Env mutational scanning (Fig 7) [84]. A requirement for both setups was to transfer SENSE-19 mutations into a full-length, replication-competent clone of JR-CSF (JR-CSF^{rc}). In the conventional PBMC setup, virus infectivity in the supernatant was monitored. The library approach depends on sequence-based detection of the infecting strains. To identify individual strains by Illumina sequencing, we included 11 mutants from the SENSE-19 panel that fall within a stretch of DNA with a length that can be covered by Illumina sequencing (S10 Fig). As controls JR-CSF wt and four glycosylation site mutants (N295A, N332A, T450A and N461A) were included.

In a first step, JR-CSF^{rc} mutants were generated and probed in two conventional neutralization setups, on PBMC and on TZM-bl cells. The results were compared to the setup with JR-CSF mutants as pseudoviruses on TZM-bl cells (Fig 6). Overall, we observed a similar pattern for the three assay systems with much stronger variations in potency across the mutant panel for weak-nAbs compared to bnAbs (Figs 6, S8 and S9). Only modest differences
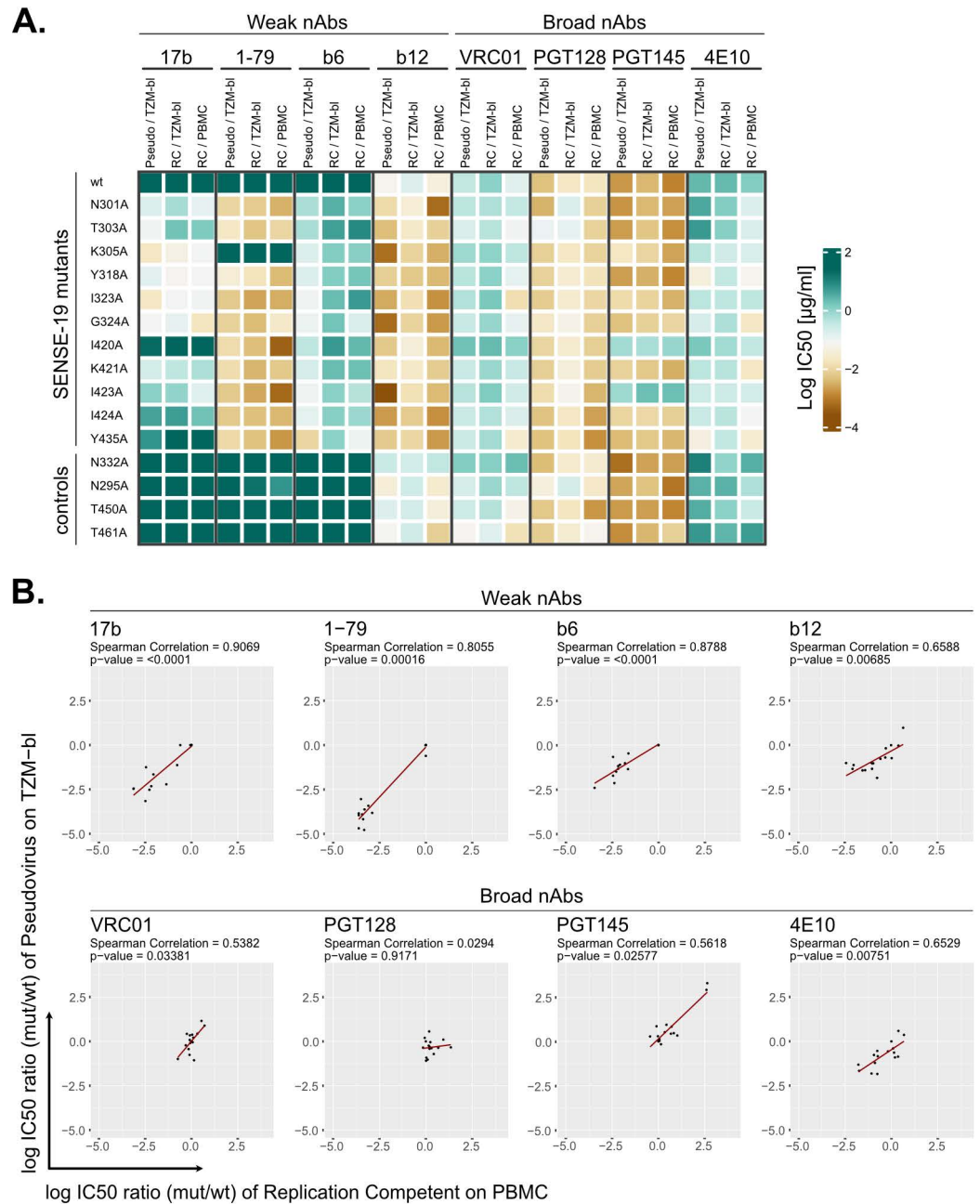
Fig 6. The generalized neutralization sensitivity phenotype is equivalent in different assay formats. JR-CSF wt virus and Env mutants were tested for neutralization sensitivity in three assay formats differing in the virus/cell combination: JR-CSF pseudovirus/TZM-bl, JR-CSFrc/TZM-bl, JR-CSFrc/PBMC. **A.** Heatmap comparing IC50 values from the three assay types. Titrations in the pseudovirus assay were performed once, except for the JR-CSF wt reference (n ≥ 4). Titrations in the JR-CSFrc/TZM-bl assay were set up in triplicates. For the JR-CSFrc/PBMC assay results are shown from one of two independent experiments set-up in triplicate for each mAb respectively. **B.** Spearman correlation of shifts in neutralization sensitivity (log IC50 ratio (mutant/wt)) between the JR-CSFrc/PBMC and JR-CSF pseudovirus/TZM-bl assays (corresponding to data shown in S8A Fig).

https://doi.org/10.1371/journal.ppat.1012825.g006

between the PBMC based assay and the two TZM-bl assays were apparent. Notably, while IC50s for most Abs correlated between the three assays (S9 Fig), Abs tended to be less potent
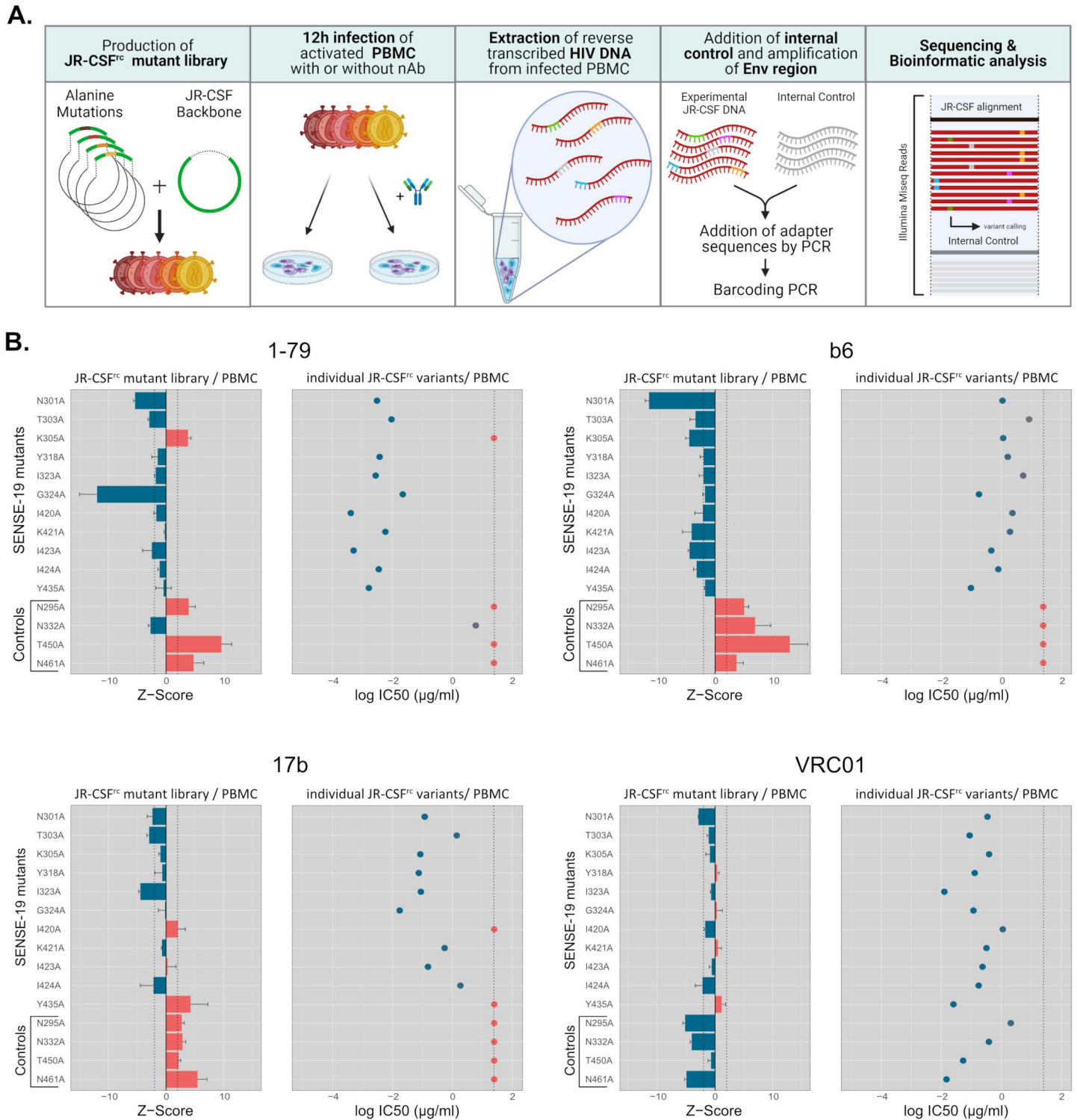
Fig 7. Validation of a virus mini-library neutralization assay for mAb fingerprinting with sequencing-based readout. The virus mini-library comprised 15 JR-CSF^rc mutant viruses including 11 of high generalized neutralization sensitivity from the SENSE-19 panel and 4 PNGS mutants (controls). Wt JR-CSF^rc was also included as reference. **A.** Schematic explaining the assay set-up and readout by Illumina sequencing. **B.** Comparison of results from the virus mini-library neutralization assay with a separately conducted PBMC based assay format testing JR-CSF^rc mutants individually against four different antibodies. Results indicating resistance and sensitivity to a nAb are colored red and blue respectively. Left panels for each Ab: Enrichment and depletion of mutant viruses in the mini-library in presence (25 μg/ml) versus absence of Ab are depicted as Z-scores (error bars: STD), with Z-score (Env variant y)$_{\text{replicate z}}$ = (arF(Env variant y)$_{\text{replicate z with Ab}}$ − mean arF(Env variant y)$_{\text{without Ab}}$)/

standard deviation arF(Env variant y) $_{without\ Ab}$, wherein arF(Env variant y) is the relative read frequency of Env variant y after adjustment according to the proportion of total JR-CSF reads versus total of reads including the internal control recovered (for details see materials and methods). A positive Z-score indicates enrichment and therefore resistance to the Ab, a negative Z-score indicates depletion and therefore sensitivity to the Ab (n = 3). The dotted lines indicate the threshold at which the enrichment/depletion in presence versus absence of antibody exceeds two times the standard deviation of read frequencies in absence of antibody (Z-scores = 2 and −2). Right panels for each Ab: Resistance of individually tested mutants in the PBMC-based assay was attributed if the IC50 was above 25 µg/ml (dotted line).

https://doi.org/10.1371/journal.ppat.1012825.g007

in the JR-CSF^{rc}/TZM-bl setup (Figs 6A and S8B). Moreover, IC50 ratios (mut/wt) correlated for most Abs between the JR-CSF/TZM-bl and JR-CSF^{rc}/PBMC formats (Fig 6B). Correlations tended to be less strong for bnAbs (in particular PGT128) which likely is a result of the bnAbs low variability in potency paired with the inherent variability of PBMC-based assays.

To probe the JR-CSF mutants in the library approach (Fig 7) individually propagated virus stocks were pooled into a library and used to infect stimulated PBMC in presence and absence of nAbs. Unlike in conventional neutralization assays, where nAb activity is probed over a wide concentration range, a single, high-dosed concentration of mAb was used in this library neutralization assay (25 µg/ml). Twelve hours post infection, DNA was isolated from the PBMC cultures and the Env region chosen for monitoring was PCR amplified from reverse transcribed non-integrated viral DNA using barcoded primers. A DNA fragment derived from a plant-gene flanked by the same primer binding sites used for Env-enrichment was added to each sample as an internal control. The amplified DNA from antibody treated and non-treated samples together with the combined internal control was sequenced by Illumina Mi-seq, and individual reads were attributed to the internal control, different mutants or the wt Env using the previously established pipeline VirVarSeq [85]. The frequency of observed reads of each individual Env mutant were used to calculate Z-scores. A positive Z-score indicates relative enrichment of the Env in presence versus absence of a nAb and thus resistance, a negative Z-score indicates sensitivity (Fig 7). We probed the feasibility of this assay format with three weak-nAbs (b6, 1–79 and 17b) and bnAb VRC01. The library setup yielded results in agreement with the TZM-bl pseudovirus assays (Fig 6A) and separate inhibition assays conducted with individual replication competent Env variants on PBMCs (Fig 7B). Resistant mutants were enriched in the library in the presence of Abs 1–79, b6 and 17b while most SENSE-19 mutants were depleted or remained at similar level as when no Ab was present (Fig 7B). In contrast, all mutants were sensitive to VRC01 and by consequence none of them was enriched. We therefore conclude that the translation of the SENSE-19 screen to a library-based screen on PBMC is feasible and has potential for screens where a qualitative readout is useful. This approach may be particularly useful, when a large number of mutant and naturally evolved Envs are combined into a screening library. Overall, the comparison of PBMC and TZM-bl assay systems highlighted that screening with SENSE-19 mutants can be integrated in the assay format of choice and provides information on the tolerance of inhibitors to trimer opening.

Discussion

The majority of bnAbs are known for their capacity to engage the closed Env trimer but, in accordance with their activity against diverse viruses, must also harbor a considerable capacity to cope with the conformational variability of Env [20,21,86,87]. In vivo, the inherent conformational heterogeneity of Env among viral quasispecies, with closed and incompletely closed Env conformations, can have a major impact on neutralization efficacy [12,26–31]. For use in prevention and treatment, bnAbs with consistent efficacy across genetically and structurally divergent Env variants are needed. Identification of bnAbs with high tolerance to Env conformational changes may aid in the selection of candidate bnAbs for clinical use. Here, we

systematically investigated the effect of Env conformational variation on bnAb activity. Generalized virus neutralization sensitivity has been associated with more frequent sampling of Env downstream conformations [17,20]. In agreement, surveying the CATNAP database we found that weak-nAbs are more potent against Tier-1 viruses, which more frequently sample downstream conformations in the absence of CD4, compared to higher tiered viruses. Interestingly, some bnAbs with different epitope specificities also showed higher potency against Tier-1 viruses although this effect appeared less pronounced (Fig 1).

To capture the impact of Env conformational variability on Ab neutralization we sought to assemble Env mutants that can serve as indicator panel for neutralization screens. Screening 126 JR-CSF gp120 mutants we defined 30 mutants that displayed a generalized enhanced neutralization sensitivity against plasma from PWH and weak-nAbs. These mutants displayed a lower stability of the closed conformation in comparison to wildtype leading to enhanced exposure of CD4-induced epitopes as demonstrated by cell-surface Env staining and neutralization sensitivity to Abs and inhibitors with post-attachment activity.

While all neutralization sensitivity conferring mutations investigated here were located within gp120, they also enhanced sensitivity to bnAbs targeting the MPER which are known to require an open Env conformation for binding [8,33,37]. Of note, as documented by other studies, mutations in gp41 can also induce a generalized neutralization sensitivity [88–91], illustrating the functional cross-talk between the gp120 and gp41 subunits. In agreement with the fact that prolonged periods of virus preincubation with MPER mAbs enhances neutralization [55], more frequent spontaneous sampling of open Env and/or altered entry process kinetics may lead to enhanced sensitivity to MPER bnAbs. More generally, spontaneous trimer opening and prolonged exposure of CD4-triggered conformations will benefit all inhibitors with post-attachment activity.

To provide a screening tool to monitor the effect of Env stability modulations on neutralization efficacy we introduced the SENSE-19 mutant panel which compares Ab activity against 19 JR-CSF Env variants with generalized neutralization sensitivity to wildtype JR-CSF (Fig 5). While bnAbs overall were less affected by increased trimer flexibility than weak-nAbs, scoring by the SENSE-19 panel provided insights on bnAb activity upon trimer opening. Increased potency against the SENSE-19 panel compared to JR-CSF wt was common among bnAbs with post-CD4 attachment activity. A second group of bnAbs tolerated SENSE-19 mutations well, with only modest potency changes compared to wt. This tolerance was achieved by several CD4bs bnAbs (VRC01, VRC07-523, 1NC9 and N49P7) and the interface bnAb PGT151. A third group of bnAb reactivity was signified by a loss in activity on SENSE-19 in agreement with their dependence on a stable closed trimer conformation for optimal binding. This group included bnAbs 3BNC117, NIH45-46, PGV04, PGDM1400 and PGT145. Notably, while they lost in potency against SENSE-19, they on average more potently neutralized Tier 1A than Tier 2 viruses according to CATNAP database data (Fig 1B). The discrepancy in activity against SENSE-19 and Tier 1A, both groups comprising generally open, neutralization-sensitive Envs, supports that SENSE-19 mutants sample different Env conformational intermediates than Tier 1A viruses. Unlike lab-adapted Tier 1A Envs containing multiple mutations, the SENSE-19 mutants are single-point mutants of a primary Env, representing Env variants that can occur randomly at any time among viral quasispecies thus representing a broad spectrum of Env heterogeneity that can emerge in vivo.

To identify the most informative mutants for the assessment of bnAb conformational tolerance among the SENSE-19 mutants we conducted a random forest analysis to create SENSE panels including 6 and 12 mutants, respectively. The selected SENSE-6 and SENSE-12 panels performed as well as SENSE-19 in assessing bnAb conformational tolerance and are recommendable when higher sample throughput is required.

A limitation of the current SENSE-19 panel is that it requires that the bnAb investigated neutralizes wildtype JR-CSF. To enable also such nAbs to be typed, creating a SENSE panel in alternate primary Env background would be necessary. We consider this feasible, but as the SENSE mutant analysis in BG505 has shown, not all Envs may be equally suitable. In any chosen Env, it will be necessary to define individual mutations that confer neutralization sensitivity and, as a panel, provide the same structural heterogeneity as in JR-CSF. SENSE-panels in the context of different Env subtypes would be of general interest to gauge the conformational Env heterogeneity across HIV subtypes.

The need to screen bnAbs considered for therapeutic use in assays using PBMC has been increasingly discussed in recent years as some differences in efficacy between PBMC infection of replication competent viruses and TZM-bl infection with pseudoviruses may exist that are relevant for in vivo use [76–81,83]. Considering the genuine complexity of PBMC neutralizations due to donor cell variability in susceptibility to HIV-1 infection and the low potential of PBMC assays for high sample throughput, we considered a SENSE library approach with a NGS readout as a possible alternative. In the present study we show that this approach is in principle feasible, and may be developed into a neutralization assay format beyond studies on SENSE-19.

Collectively, the SENSE-19 screens provided compiled information on breadth, potency, and structural dependencies, and in particular, distinguished bnAbs with post-attachment activity. We postulate a utility of SENSE-19 as an extension to existing multi-subtype Env panels used for neutralization breadth and potency determination as it offers a framework for classifying bnAb activity based on structural changes in the HIV-1 Env protein. Virus quasispecies contain many variants with subtle sequence changes inflicting modest to large conformational changes and bnAbs used for prevention need to be able to combat them. We therefore consider the ability to cope with conformational variability as a feature of bnAbs that could provide relevant additional information about their breadth and thus provide an additional selection criterion to ascertain that the best bnAb or the best combination of bnAbs is moved forward in development.

Materials and methods

Ethics statement

All analyzed plasma samples (S2 Table) were derived from specimens stored in the biobanks of the Swiss HIV Cohort study (SHCS) and the Zurich Primary HIV Infection Study (ZPHI). The Swiss HIV Cohort Study (SHCS) is a prospective, nationwide, longitudinal, non-interventional, observational, clinic-based cohort with semi-annual visits and blood collections, enrolling all HIV-infected adults living in Switzerland [105]. The SHCS is registered under the Swiss National Science longitudinal platform: http://www.snf.ch/en/funding/programmes/longitudinal-studies/Pages/default.aspx#Currently%20supported%20longitudinal%20studies. Detailed information on the study is openly available on http://www.shcs.ch.

The Zurich Primary HIV Infection study (ZPHI) is an ongoing, observational, non-randomized, single center cohort founded in 2002 that specifically enrolls patients with documented acute or recent primary HIV-1 infection (www.clinicaltrials.gov; ID NCT00537966) [106].

The SHCS and the ZPHI have been approved by the ethics committee of the participating institutions (Kantonale Ethikkommission Bern, Ethikkommission des Kantons St. Gallen, Comité départemental d'éthique des spécialités médicales et de médecine communautaire et de premier recours, Kantonale Ethikkommission Zürich, Repubblica e Cantone Ticino - Comitato Ethico Cantonale, Commission cantonale d'éthique de la recherche sur l'être humain,

Ethikkommission beider Basel for the SHCS and Kantonale Ethikkommission Zürich for the ZPHI) and written informed consent had been obtained from all participants.

Antibodies and reagents

Reagents were kindly provided by following groups: Soluble CD4 (sCD4) comprising all four immunoglobulin domains [92,93] and CD4IgG2 [94] by W. Olson (Progenics Pharmaceuticals Inc., Tarrytown, New York, USA); monoclonal antibodies (mAbs) VRC01, PGV04 [39] by J. Mascola (NIAID, NIH, Bethesda, USA); mAbs b12 [95], b6 [96], PG9 and PG16 [54], PGT121, PGT128, PGT130, PGT135 and PGT145 [38] and PGDM1400 [97] by D. Burton (The Scripps Research Institute, La Jolla, USA); mAbs 2G12 [98], 2F5 [99], 4E10 [100,101] and 1F7 [102] by H. Katinger (Polymun, Vienna, Austria); mAbs 1–79, 3BNC117 and NIH45-46 [103] by M. Nussenzweig (Rockefeller University, New York, NY, USA); 447-52D [104] by S. Zolla-Pazner (Icahn School of Medicine at Mount Sinai, New York, NY, USA); 10E8 [37], 48D and 17b via the NIH AIDS Research and Reference Reagent Program, Division of AIDS, NIAID, NIH. Soluble CD4 containing the two amino-terminal immunoglobulin domains (sCD4-183) was expressed in E. coli and purified as described [25]. An overview is provided in S3 Table.

Cells

293-T cells were obtained from the American Type Culture Collection. The TZM-bl cell line was obtained from NIH ARP. Both cell lines were cultivated in DMEM medium supplemented with 10% fetal calf serum (FCS) and 100 µg/ml streptomycin and 100 U/ml penicillin (P/S) (referred to as cell culture medium hereafter). All cell culture reagents were obtained from Gibco (Thermo Scientific, Waltham, USA).

PBMC were purified from buffy coats from anonymous blood donations from healthy individuals obtained by the Zurich Blood Transfusion Service (http://www.zhbsd.ch/) under a protocol approved by the local ethics committee. PBMC from three individual donors were CD8+ T-cell depleted using Rosette Sep cocktail (StemCell Technologies Inc.), pooled, split into three parts and incubated for three days with either 5 µg/ml PHA, 0.5 µg/ml PHA or anti-CD3 mAb OKT3 in RPMI 1640 medium (10% FCS, 10 U/ml IL-2, glutamine and 1% penicillin-streptomycin) [107].

Viruses

The plasmid collection of JR-CSF env alanine mutants [38,53,54] and was a kind gift from D. Burton (The Scripps Research Institute, La Jolla, USA). The BG505.W6M.ENV.C2 [108] encoding source plasmid was obtained from the NIH AIDS Research and Reference Reagent Program. BG505 Env mutants and additional JR-CSF Env mutants were generated using the QuikChange II XL Site-Directed Mutagenesis Kit (Agilent, Santa Clara, USA) according to the manufacturer's instructions. A BG505 Env mutant with V1V2 deletion was generated as described previously [11]. Pseudotyped virus production was performed by co-transfection of 293T cells with Env expression plasmid and HIV vector pNLluc-AM carrying a luciferase reporter cassette (provided by A. Marozsan and J. P. Moore) as described previously [81]. Information on the composition of a 40 virus panel used to assess mAb breadth and potency can be found in S4 Table.

To generate replication competent mutant viruses, the JR-CSF Env encoding fragments containing the desired alanine substitutions were ligated in-frame into a replication competent JR-CSF infectious molecular clone (pYK-JRCSF obtained through the NIH ARP, catalog no. 2708 [109]) using InFusion technology (Takara Bio Inc., USA) according to instructions

by the manufacturer. Replication competent virus was produced by transfection of 293T cells with pYK-JRCSF based vectors analogous to the production of pseudotyped virus [81].

Neutralization assay using Env-pseudotyped virus

The neutralization sensitivity of Env-pseudotyped viruses against mAbs and plasma from people living with HIV-1 (PWH) was evaluated on TZM-bl reporter cells in 384 well plates. Virus input was diluted with cell culture medium aiming for a luciferase reporter readout of 500,000–1,000,000 relative light units (RLU) per well measured on an EnVision luminometer (Perkin Elmer, Waltham, USA) in the absence of inhibitors. The antibody concentration (IC50) or reciprocal plasma titer (ID50) causing 50% reduction in viral infectivity were calculated by fitting the data to sigmoid dose–response curves (variable slope) using Prism (Graph-Pad Software). If 50% inhibition was not achieved at the highest or lowest concentration, a greater than or less than value was recorded.

Two different assay setups were established. To verify their comparability, PG128, PGT145, 10E8 and 2G12 were tested in both setups over the whole JR-CSF panel (N = 126) and no systemic discrepancies were identified.

In the first set up, serial dilutions of inhibitors and PWH plasma in cell culture medium supplemented with 50mM HEPES were prepared robotically in 384 well plates (60 μl per well) (Corning, Corning, USA). This was followed by adding 20 μl per well of pseudovirus suspension. After 1–2 hours incubation at 37 °C, 20 μl TZM–bl cell suspension at 150'000 cells per ml density in cell culture medium supplemented with 60 μg/ml DEAE-Dextran were pipetted robotically to each well and the plates were incubated for 48 hours at 37 °C before proceeding to the readout of luciferase signal on an EnVision luminometer (Perkin Elmer, Waltham, USA) as described [81].

In an alternative assay format serial dilutions of inhibitors in cell culture medium (40 μl per well) were added to 40 μl of virus suspension in 384 well plates. After 1–2 hours incubation at 37 °C 50 μl of the virus-inhibitor mixture were added to pre-seeded TZM-bl cell cells (384 well plates, 6000 cells/well in 30μl culture medium supplemented with 26.6 μg/ml DEAE-Dextran) and the plates were incubated for 48 hours at 37 °C before readout of the luciferase signal on an EnVision luminometer (Perkin Elmer, Waltham, USA) as described [81].

Neutralization data of bnD.1, bnD.2, bnD.3 and mAb 447-52D on the full JR-CSF mutant panel was reproduced from Friedrich et al [51]. Neutralization data of bnD.4, bnD.8, bnD.9 as well as mAbs PGT128 and 17b on strongly neutralization sensitive Env mutants was reproduced from Glögl et al [68].

Neutralization assay using replication competent HIV

In addition to the pseudovirus neutralization assay performed on TZM-bl cells, replication competent virus was used to infect TZM-bl cells or PBMC in presence and absence of an inhibitor. To determine relative infectivity the individual replication competent virus stocks were first titrated on TZM-bl cells (seeded the previous day in a 384 well plate at 6000 cells/well density in 30 μl culture medium supplemented with 26.6 μg/ml DEAE-Dextran). The plate was incubated for 48 hours at 37 °C before readout of the luciferase signal analogous to the procedure when using pseudovirus detailed above. As replication competent viruses are cytolytic for TZM-bl cells at high concentrations, this allowed to determine the dilution of the viral stock at which the TZM-bl cells survive for at least 3 days while ensuring high signal over background during readout. This virus dilution was not only used for inhibition assays of replication competent virus on TZM-bl cells, but also as input for the PBMC-based neutralization assay in 384 well plates.

For inhibition assays on TZM-bl cells, replication competent virus was titrated with inhibitor in triplicates, pre-incubated for 1 h at 37 °C and 30 μl/well of virus-inhibitor mix were then transferred onto TZM-bl cells seeded the previous day (384 well plate, 6000 cells/well in 30 μl culture medium supplemented with 26.6 μg/ml DEAE-Dextran). The plate was incubated for 48 hours at 37 °C before readout of the luciferase signal analogous to the procedure when using pseudovirus detailed above.

For inhibition assays on PBMC, replication competent virus was titrated with inhibitor in triplicate, pre-incubated for 1h at 37 °C and 30 μl/well of virus-inhibitor mix were then transferred onto PBMC (seeded at 1.5×10^6 cells/ml density in 30 μl/well RPMI 1640 with glutamine supplemented with 10% FCS, 100 U/ml IL-2, and 1% penicillin-streptomycin). After incubation for 7 days at 37 °C, plates were spun down at 450 g for 2 min and 30 μl/well of supernatant were transferred onto TZM-bl cells (seeded the previous day in a 384 well plate at 6000 cells/well density in 30 μl culture medium supplemented with 26.6 μg/ml DEAE-Dextran). After a further 24–72 hours of incubation infection was quantified by luciferase reporter readout as described for the pseudovirus assay to assess virus inhibition by antibody relative to wells without antibody. Additional wells which received the double amount of virus input in the PBMC-step were used as control to ensure that cytolysis was not affecting the assay.

Sequencing based evaluation of neutralization assay with JR-CSF point mutant mini-library

To prepare the mini-library of replication competent JR-CSF Env point mutant viruses, individually prepared stocks of replication competent mutant viruses were mixed at equal volume. For the neutralization assay with this virus library PBMC were seeded at 3×10^6 cells/ml in 250 μl RPMI 1640 with glutamine supplemented with 10% FCS, 100 U/ml IL-2, and 1% penicillin-streptomycin on 24-well culture plates. 125 μl of the virus library were preincubated either with or without 125 μl inhibitory agent diluted in cell culture medium aiming for a final concentration of 25 μg/ml after transfer of the mix onto PBMC. Each condition was set up in triplicates. The mixture of virus library and inhibitor was pre-incubated for 1h at 37 °C and then transferred onto the seeded PBMC. 12 hours post-infection the cells were spun down at 16'000 g for 10 min and washed with PBS. The reverse-transcribed non-integrated viral cDNA was then extracted from PBMC using QIAprep Spin Miniprep Kit (Qiagen, Aarhus, Denmark). Samples were handled with frequent glove and pipette tip changing while any solution used was aliquoted to prevent cross contamination [110,111]. As an internal control, 1 μl at 1 pg/ml of a custom synthesized 544 base-pair sized dsDNA fragment (Twist Bioscience, South San Francisco, California, USA) containing 500 base-pairs of a plant-gene (EMB2768 – Farinopsis Salesoviana) flanked on each side by one of the two primer binding sites used for amplification of Env-fragments (described below) was added to each sample. In a first PCR (see S5 Table) amplification of Env fragments covering all alanine substitutions in the virus mini-library (and the internal DNA control fragment) was done with Env specific forward and reverse primers of three different lengths containing adapter sequences at the 5' end.

Forward primers: CTTTCCCTACACGACGCTCTTCCGATCT(N)$_{6,7,8}$AACCATA-ATAGTACAGCTGAATGAATC.

Reverse primers: GGAGTTCAGACGTGTGCTCTTCCGATCT(N)$_{6,7,8}$TCTGAAGATCTC-GATCTCACTCT.

The differing length of the primers artificially increases diversity of the otherwise highly similar amplicons for efficient MiSeq sequencing. In addition, 5 random nucleotides between

the adapter-region and binding region of the primers were added to facilitate cluster generation during illumina amplification of reads. The forward and reverse primers of different lengths were used at 3.33 μM concentration each, to result in 10 μM forward and reverse primer mixtures.

The DNA was then purified from the PCR reactions using AMPure XP beads (Backman Coulter Life Sciences, Indianapolis, USA) at a 1:1 ratio (vol/vol) as recommended in the instructions by the manufacturer. After the clean-up, a 2nd PCR was performed (see S5 Table) to barcode the individual samples using Index primers (TruSeq HT Kits, Illumina Inc., San Diego, California, USA) able to bind the adapter-region established during the previous PCR.

After PCR dsDNA concentration in samples was measured with the QuantiFluor system (Promega). The samples were subsequently diluted to 4 nM concentration and twenty-four samples were mixed together in equal parts. The Ilumina sequencing used a MiSeq Reagent Kits v2 (500 cycles) and was executed based on manufacturer's instructions.

For evaluation individual reads were attributed to the internal control, different Env mutants or the wt Env using VirVarSeq [85]. Then, the relative frequencies of each Env variant ($rF(\text{variant } y)_{rep\ z}$) computed by VirVarSeq (controlled for position-specific read quality) in samples treated or not with antibody were transformed into adjusted relative frequencies ($arF(\text{variant } y)_{rep\ z}$) taking into account the number of reads corresponding to the internal control.

$$arF\left(variant\ y\right)_{rep\ z} = rF\left(variant\ y\right)_{rep\ z} \times \frac{n\left(JRCSF\ reads\right)_{rep\ z}}{n\left(JRCSF\ reads\right)_{rep\ z} + n\left(EMB2768\ reads\right)_{rep\ z}}$$

rep z: replicate 1, 2 or 3.

n (JRCSF reads): total number of reads aligned to JR-CSF reference by VirVarSeq.

n (EMB2768 reads): total number of reads aligned to plant reference by VirVarSeq.

Based on the adjusted relative frequencies of reads, Z scores were calculated for individual Env variants of each experimental replicate as follows:

$$Z\ score\left(variant\ y\right)_{rep\ z} = \frac{arF\left(variant\ y\right)_{rep\ z\ with\ Ab} - mean\ arF\left(variant\ y\right)_{in\ absence\ of\ Ab}}{standard\ deviation\ from\ mean\ arF\left(variant\ y\right)_{in\ absence\ of\ Ab}}$$

Wherein the mean adjusted relative frequency of an Env variant in absence of antibody is:

$$mean\ arF\left(variant\ y\right)_{in\ absence\ of\ Ab} = \frac{arF\left(variant\ y\right)_{rep\ 1} + arF\left(variant\ y\right)_{rep\ 2} + arF\left(variant\ y\right)_{rep\ 3}}{n\left(reps\right)}$$

The internal control allows the comparison of read frequencies from Env variants in presence and absence of Ab and is particularly important in case the majority of viruses in the mini-library is sensitive to the Ab.

Flow cytometric analysis of antibody binding to cell surface-expressed HIV-1 Env

10^5 293T cells per well were seeded in 1 ml cell culture medium in 12-well tissue culture plates and incubated at 37 °C. 24 hours later, cells in each well were transfected with a total of 1 μg DNA (Env-expression plasmid and pCMV-*rev* expression helper plasmid in 4:1 ratio) mixed with 3 μg 25 kDa linear PEI (Polysciences Inc., Warrington, USA) in 200 μl 150 mM NaCl.

After settling the DNA-PEI complexes by a short spin (3 min, RT, 300 g) the cells were incubated 36 hours at 37 °C. All subsequent steps were carried out at room temperature. Cells were harvested, wells transfected with the same Env-plasmid pooled, and distributed into 96-well round bottom tissue culture plates as individual staining reactions (cells from one 12-well were split into four staining reactions). For each staining reaction cells were washed once with 200 µl FACS buffer (DPBS (Gibco) with 2% FBS, and 2 mM EDTA) and stained for 20 min in 15 µl of FACS buffer with 10 µg/ml of primary antibody in the presence or absence of sCD4-183. After washing twice with 200 µl FACS buffer the cells were incubated in 30 µl of FACS buffer for 20 min with 1:1000 diluted APC-conjugated F(ab')$_2$ fragment goat anti-human IgG (Jackson ImmunoResearch, West Grove, USA). Following two further washes with FACS buffer the cells were resuspended in 100 µl FACS buffer with 0.1 µg/ml propidium iodide (BD Pharmingen). Flow cytometry analysis was performed on a FACSVerse system (BD biosciences, San Jose, USA). Arithmetic mean of APC fluorescence intensity was calculated for Propidium Iodide negative single cell population as a measure of primary antibody binding to the live cells in each staining reaction.

Env mutants were devided into two groups showing enhanced 17b binding in absence of sCD4 or not compared to JR-CSF wt Env (threshold 10% of normalized maximal staining in presence of sCD4). To determine the area under the normalized MFI curves on a log-x-scale, all sCD4 concentrations (in uM), at which binding was measured, were enhanced by "0.01", such that MFI measurements in the absence of sCD4 could be included.

Entry capacity

The entry capacity of Env variants was assessed by measuring the infectivity of Env pseudoviruses on TZM-bl cells in the presence of 10 µg/ml diethylaminoethyl-dextran (DEAE), normalized to the gp120 and p24 content of the pseudovirus stocks. Pseudovirus stocks using all SENSE-19 JR-CSF Env mutants and JR-CSF wt Env were generated as described above on the same day using the same stock of HIV-1 backbone plasmid NL-lucAM, polyethylenimine (PEI) max transfection reagent and 293 T cells. Cell culture supernatants containing pseudovirus were harvested three days later and aliquots were frozen at −80 °C. Infectivity, gp120 and p24 content were measured in parallel for all Env variants and measurements were performed in biological duplicates. For the infectivity measurements, pseudovirus serial dilutions were added to TZM-bl cells and luciferase activity (relative light units (RLU)) was measured three days post-infection using Luciferase assay reagent (Promega, USA). In parallel, aliquots of pseudovirus stocks were inactivated with 1% Empigen final concentration and serially diluted in TBS/1% Empigen. Gp120 (in-house produced affinity-purified JR-FLgp120 protein) and p24 (AG 6054, Aalto Bioreagents, Ireland) standards were prepared accordingly. Gp120 and p24 content of virus lysates was measured by ELISA as previously described [112]. Briefly, gp120 was captured by sheep anti-gp120 antibody (D7324, Aalto Bioreagents, Ireland) coated the day before to the surface of high-binding 384-well ELISA plates (corning). Biotinylated human anti-gp120 2G12 mAb was used as primary detection antibody, alkaline-phosphatase-conjugated streptavidin as secondary detection reagent. For the p24 ELISA setup, p24 was captured on sheep anti-p24 antibody (D7320, Aalto Bioreagents, Ireland) coated 384-well plates and detected using alkaline-phosphatase-coupled antibody BC1071-AP (Aalto Bioreagents, Ireland). Gp120 and p24 content were then interpolated from standard curves of recombinant gp120 and p24 respectively or determined relative to the gp120 and p24 content of JR-CSF wt Env pseudovirus. The obtained infectivity (RLU/µL) values for each stock were normalized to the gp120/p24 concentrations of the respective stock.

Bioinformatics and software

To evaluate whether SENSE-19 could be reduced to a smaller number of mutants, we assessed the variable importance (mean decrease accuracy) of each mutant in a random forest predicting the conformational preference of each antibody (open, close, none as in Fig 5C), as determined by SENSE-19. We then selected the top 6 and top 12 mutants based on visual inflection points in the variable importance curve (S7E Fig). We computed SENSE-6 and SENSE-12 scores on the 6-mutant and 12-mutant panels respectively, similarly as the SENSE-19 score (i.e., log value of the IC50 medians). Using the same thresholds as for SENSE-19 (−0.2 and 0.2), we then verified whether all antibodies were classified in the same categories as predicted by SENSE-19. Analyses were conducted in R version 4.3.1 with the package randomForest.

To analyze Ilumina sequencing data from the JR-CSF library, VirVarSeq [85] was used to calculate the frequency of wildtype and mutant Envs as well as the internal control in presence or absence of an inhibitor. Sequences were trimmed using SeqTK [113] to remove residual, random nucleotides introduced to support Miseq amplification of reads.

Figs 1, 2, 3C, 4C, 5, 6, 7B, and S1, S2C, S3B, S5, S7, S8 were produced using the R packages ggplot2 [114], heatmaply [115], tidyverse [116] and Hmisc [117]. Figs 3A, 4B and S2D and S4B were produced in GraphPad Prism 10 (GraphPad Software, Boston, Massachusetts, USA). FACS-generated data was processed using FlowJo™ Software v10.9 (BD Life Sciences). Fig 4D was designed using PyMOL v2.5 (https://pymol.org/2/). Biorender (Subscription model, Canada) was utilized to make Figs 4A and 7A. Affinity Designer (SerifEurope, UK) was used to finalize all figures.

Supporting information

S1 Fig. Characterizing the general neutralization sensitivity of JR-CSF envelope point mutants. The general neutralization sensitivity of 126 JR-CSF envelope (Env) mutant pseudoviruses was determined in a TZM-bl based assay using **A.** a set of 16 PWH plasma from chronic infection (eleven subtype B infected, five with non-B subtypes). **B.** ID50s for a subset of 5/16 plasma that did not inhibit JR-CSF wt Env at an inhibitory dilution ID50 = 100, the minimal dilution probed (four plasma samples from subtype B, one from non-subtype B infected individuals). **C.** ID50s for five plasma samples from PWH chronically infected with non-subtype B HIV-1 (subtype of infection in parentheses). Three plasma samples neutralized JR-CSF wt, two did not. (Boxplots show center line: median; box limits extend from the 25th to 75th percentiles; whiskers indicate minimum and maximum values). Mutants with high and moderate general neutralization sensitivity as assigned by the analysis presented in Fig 2A are colored in red and blue respectively. S2 Table provides an overview of the plasma samples used. Titrations of each plasma on all viruses was done once, except for the JR-CSF wt reference (n = 4).
(PDF)

S2 Fig. Characterizing the exposure of the co-receptor binding site by neutralization sensitive JR-CSF Env mutants. Opening of 293T cell surface expressed Envs by increasing concentrations of sCD4-183 is monitored by flow cytometry after staining with mAb 17b, directed against a CD4-induced epitope similar to the CCR5 co-receptor binding site. **A.** Example to illustrate the gating strategy applied during analysis by flow cytometry. **B.** Histograms showing the 17b staining obtained for each Env mutant. **C.** Spearman correlation between 17b neutralization sensitivity of JR-CSF wildtype and mutant viruses and 17b binding according to Fig 4B. In comparison to Fig 4C mutations directly affecting 17b binding [65] were included. **D.** Env mutants T303A and T303I are differentiated by 17b binding at baseline,

i.e., in absence of sCD4, and by their propensity to expose the 17b epitope with increased concentrations of sCD4-183. The bar graph on the right shows corresponding area under the MFI curve values. All titrations were performed once.
(PDF)

S3 Fig. Sequence conservation and structural interactions in amino acid positions associated with general neutralization sensitivity. A. Alanine-substitutions leading to moderate (blue) or high (red) generalized neutralization sensitivity of the JR-CSF Env were mapped onto the trimeric closed prefusion structure of the closely related JR-FL Env ectodomain (PDB: 5FYK; V1V2: yellow, V3: orange, β20-β21: brown, gp120: light grey, gp41: dark grey). The enlargements show interactions identified in the structure mediated by the side chains of amino acids critical for neutralization sensitivity (D167 in V2: interprotomer salt bridges to T128 and R192 in V2; K305 in V3: intraprotomer salt bridge to E172 in V2; Y435 in β20-β21: intraprotomer hydrogen-bonds to Y318 and T319 in V3). **B.** Conservation of all 125 amino-acid positions mutated in the full JR-CSF Env mutant panel. A superfiltered web alignment (available from the Los Alamos National Laboratory database, http://www.lanl.com) of diverse HIV-1 Env sequences (6084 Env sequences from group M including CRFs) was downloaded for the most recent year available (2021) and all relevant amino acid positions were analyzed for their conservation. Residues associated with high (red) and moderate (blue) general neutralization sensitivity are indicated.
(PDF)

S4 Fig. Analyzing the propensity of BG505_T332N (wt) envelope and mutants to adopt the CD4-induced conformation. Titration of 293T cell surface expressed BG505 wt envelope and mutants with sCD4-183. The induced opening of the Env trimer was monitored with V3-crown directed mAb 1–79 and analyzed by FACS. **A.** Histograms showing mAb 1–79 staining. **B.** Dose-response curves for all Envs tested. The reference envelope BG505_T332N and the R308A mutant (the corresponding JR-CSF mutant has a wt-like phenotype) are colored in black and grey, respectively. BG505 mutants in red reproduce the enhanced propensity to adopt the CD4i state observed for corresponding JR-CSF mutants, the mutants in purple do not. A V1V2 deleted BG505 T332N envelope was included as control (dashed red line). K305A and I307A are 1–79 knock-out mutants (brown). MuLV envelope was used as control for unspecific staining (brown). The two panels show the same data without (left) and with (right) normalization to the highest signal obtained for each mutant respectively.
(PDF)

S5 Fig. Probing the neutralization sensitivity of selected BG505 envelope mutants. Neutralization sensitivity was determined for 17 alanine mutants based on the BG505 T332N Env (designated as wt) corresponding to JR-CSF alanine mutants with strong general neutralization sensitive phenotype using a pseudovirus assay system with TZM-bl cells. **A.** and **B.** Plots show changes in IC50 values relative to the wt envelope. A BG505 T332N Env lacking V1V2 (ΔV1V2) was included as a sensitive control. Depicted are results using **A.** CD4bs-directed, **B.** V3-crown directed (1–79), and V2-glycan directed (PG16, PGT145) Abs. **C.** ID50 values were determined for three BG505 Env mutants using 16 PWH plasma samples (13 infected with subtype B (circles) and 3 with non-subtype B (triangles) HIV). The minimal dilution of plasma tested was 1/100. For each mutant the median ID50 is indicated with a red bar.
(PDF)

S6 Fig. Hierarchical clustering analysis of JR-CSF mutant Envs. All 126 JR-CSF mutant Envs included in the full virus panel were grouped according to their changes in neutralization sensitivity compared to wt (log IC50 ratios (mut/wt)) against the antibodies indicated at the bottom.

For PWH plasma the median reciprocal ID50 ratio (mut/wt) over 11 JR-CSF wt neutralizing plasma (Fig 2A) was used. Two clusters of comprising generally neutralization sensitive mutants are highlighted in green. Mutants in bold were selected for the SENSE-19 virus panel. (PDF)

S7 Fig. Neutralization fingerprinting using generally neutralization sensitive JR-CSF Env mutants. Infectivity analysis of SENSE-19 pseudoviruses. **A.** Two independent transfections were done for each pseudovirus and each stock was titrated in duplicate on TZM-bl cells. **B.** The same stocks as in (A) were used to determine the gp120 and p24 content by ELISA. Each sample was titrated in duplicate. Data is expressed relative to pseudovirus with wildtype JR-CSF Env. **C.** Infectivity shown in (A) was normalized to gp120/p24 content shown in (B) and expressed relative to pseudovirus with wildtype JR-CSF Env. **D.** Neutralization fingerprinting of monovalent bnDs on the SENSE-19 mutant virus panel. IC50 ratios (mutant/wt) are displayed as a heatmap. **E.** Random forest analysis on all SENSE-19 mutants using data shown in Fig 5A. The analysis assesses the contribution of each mutant to the classification of bnAbs into the three categories of conformational dependence shown in Fig 5C. The combination of 6 (TOP 6), respectively 12 mutants (TOP 12) that yielded the best classification are highlighted by boxes. **F.** Comparison of SENSE-19 scores with scores obtained with the TOP 6 and TOP 12 mutant panels determined in (E).
(PDF)

S8 Fig. Probing the equivalency of the generalized neutralization sensitive phenotype in different assays formats. JR-CSF wt virus and Env mutants with and without high overall neutralization sensitivity were tested in three different assay formats. IC50 values were determined in a pseudovirus assay system with TZM-bl reporter cells and in two set-ups with replication competent virus (JR-CSF^{rc}) infecting either TZM-bl cells or PBMCs. **A.** Heatmap of log IC50 ratio (mut/wt) values. **B.** Distribution of IC50 values corresponding to data in A. Box plot indicates median (center line), 25th to 75th percentiles (box limits) as well as minima and maxima (whiskers). Titrations in the pseudovirus assay were performed once, except for the JR-CSF wt reference (n ≥ 4). Ab titrations in the JR-CSF^{rc}/TZM-bl assay were set up in triplicates. For replication competent virus on PBMCs results are shown from one of two independent experiments set-up in triplicate for each mAb respectively.
(PDF)

S9 Fig. Spearman correlations of virus neutralization sensitivity data from three different assay formats. Log IC50 values were correlated for the Abs indicated from two of three different assay formats respectively, based on data shown in Fig 6A.
(PDF)

S10 Fig. Sequencing-based evaluation of an inhibition assay using a library of replication competent viruses on PBMC. The schematic indicates the positioning of primer binding sites used to determine the composition of a replication competent virus mixture containing JR-CSF wt and point mutated envs by Illumina MiSeq sequencing.
(PDF)

S1 Table. Overview on the number of IC50 neutralization values available on CATNAP for tier-categorized strains per Ab as of October 2024 which were used to generate Fig 1.
(PDF)

S2 Table. Overview on the characteristics of plasma samples from people living with HIV (PWH) used in the study.
(PDF)

S3 Table. Overview of origin and source for all mAbs used in the present study.
(PDF)

S4 Table. Information on the composition of a 40 virus panel used to assess mAb breadth and potency.
(PDF)

S5 Table. PCR conditions used during sequencing-based evaluation of virus inhibition assays.
(PDF)

S1 Data. This Excel file contains the source data of all main and supplementary figures.
Each sheet in the file contains the data for one figure and is labelled accordingly.
(XLSX)

Acknowledgments

Author contributions

Conceptualization: Nikolas Friedrich, Peter Rusert, Alexandra Trkola.

Data curation: Caio Foulkes, Nikolas Friedrich, Branislav Ivan, Emanuel Stiegeler, Huldrych F. Günthard, Alexandra Trkola.

Formal analysis: Caio Foulkes, Nikolas Friedrich, Branislav Ivan, Emanuel Stiegeler, Carsten Magnus, Daniel Schmidt, Umut Karakus, Jacqueline Weber, Huldrych F. Günthard, Chloé Pasin, Peter Rusert.

Funding acquisition: Huldrych F. Günthard, Alexandra Trkola.

Investigation: Caio Foulkes, Nikolas Friedrich, Branislav Ivan, Emanuel Stiegeler, Carsten Magnus, Daniel Schmidt, Umut Karakus, Jacqueline Weber.

Methodology: Caio Foulkes, Branislav Ivan, Carsten Magnus.

Resources: Huldrych F. Günthard.

Supervision: Nikolas Friedrich, Peter Rusert, Alexandra Trkola.

Validation: Caio Foulkes, Nikolas Friedrich.

Visualization: Caio Foulkes, Daniel Schmidt, Chloé Pasin, Alexandra Trkola.

Writing – original draft: Caio Foulkes, Nikolas Friedrich, Alexandra Trkola.

Writing – review & editing: Nikolas Friedrich, Alexandra Trkola.

References

1. Haynes BF, Wiehe K, Borrow P, Saunders KO, Korber B, Wagh K, et al. Strategies for HIV-1 vaccines that induce broadly neutralizing antibodies. Nat Rev Immunol. 2023;23(3):142–58. Epub 2022/08/12. https://doi.org/10.1038/s41577-022-00753-w PMID: 35962033; PMCID: PMCPMC9372928

2. Paneerselvam N, Khan A, Lawson BR. Broadly neutralizing antibodies targeting HIV: progress and challenges. Clin Immunol. 2023;257:109809. https://doi.org/10.1016/j.clim.2023.109809 PMID: 37852345

3. Pihlstrom N, Bournazos S. Engineering strategies of Anti-HIV antibody therapeutics in clinical development. Curr Opin HIV AIDS. 2023;18(4):184–90. Epub 2023/05/05. https://doi.org/10.1097/COH.0000000000000796 PMID: 37144557

4. Cale EM, Bai H, Bose M, Messina MA, Colby DJ, Sanders-Buell E, et al. Neutralizing antibody VRC01 failed to select for HIV-1 mutations upon viral rebound. J Clin Invest. 2020;130(6):3299–304. https://doi.org/10.1172/JCI134395 PMID: 32182219

5. Scheid JF, Horwitz JA, Bar-On Y, Kreider EF, Lu C-L, Lorenzi JCC, et al. HIV-1 antibody 3BNC117 suppresses viral rebound in humans during treatment interruption. Nature. 2016;535(7613):556–60. https://doi.org/10.1038/nature18929 PMID: 27338952

6. Corey L, Gilbert PB, Juraska M, Montefiori DC, Morris L, Karuna ST, et al. Two Randomized Trials of Neutralizing Antibodies to Prevent HIV-1 Acquisition. N Engl J Med. 2021;384(11):1003–14. https://doi.org/10.1056/NEJMoa2031738 PMID: 33730454

7. Guttman M, Cupo A, Julien J-P, Sanders RW, Wilson IA, Moore JP, et al. Antibody potency relates to the ability to recognize the closed, pre-fusion form of HIV Env. Nat Commun. 2015;6:6144. Epub 2015/02/06. https://doi.org/10.1038/ncomms7144 PMID: 25652336; PMCID: PMC4338595

8. Harris AK, Bartesaghi A, Milne JLS, Subramaniam S. HIV-1 envelope glycoprotein trimers display open quaternary conformation when bound to the gp41 membrane-proximal external-region-directed broadly neutralizing antibody Z13e1. J Virol. 2013;87(12):7191–6. Epub 2013/04/19. https://doi.org/10.1128/JVI.03284-12 PMID: 23596305; PMCID: PMC3676106

9. Ozorowski G, Pallesen J, de Val N, Lyumkis D, Cottrell CA, Torres JL, et al. Open and closed structures reveal allostery and pliability in the HIV-1 envelope spike. Nature. 2017;547(7663):360–3. Epub 2017/07/12. https://doi.org/10.1038/nature23010 PMID: 28700571; PMCID: PMCPMC5538736

10. Reh L, Magnus C, Schanz M, Weber J, Uhr T, Rusert P, et al. Capacity of broadly neutralizing antibodies to inhibit HIV-1 cell-cell transmission is strain- and epitope-dependent. PLoS Pathog. 2015;11(7):e1004966. https://doi.org/10.1371/journal.ppat.1004966 PMID: 26158270

11. Rusert P, Krarup A, Magnus C, Brandenberg OF, Weber J, Ehlert A-K, et al. Interaction of the gp120 V1V2 loop with a neighboring gp120 unit shields the HIV envelope trimer against cross-neutralizing antibodies. J Exp Med. 2011;208(7):1419–33. Epub 2015/07/09 https://doi.org/10.1084/jem.20110196 PMID: 21646396; PMCID: PMCPMC4497647

12. Yang Z, Dam K-MA, Bridges MD, Hoffmann MAG, DeLaitsch AT, Gristick HB, et al. Neutralizing antibodies induced in immunized macaques recognize the CD4-binding site on an occluded-open HIV-1 envelope trimer. Nat Commun. 2022;13(1):732. Epub 2022/02/08 https://doi.org/10.1038/s41467-022-28424-3 PMID: 35136084; PMCID: PMCPMC8826976

13. Zhou T, Lynch RM, Chen L, Acharya P, Wu X, Doria-Rose NA, et al. Structural repertoire of HIV-1-neutralizing antibodies targeting the CD4 supersite in 14 donors. Cell. 2015;161(6):1280–92. Epub 2015/05/21. https://doi.org/10.1016/j.cell.2015.05.007 PMID: 26004070; PMCID: PMCPMC4683157

14. Haim H, Salas I, McGee K, Eichelberger N, Winter E, Pacheco B, et al. Modeling virus- and antibody-specific factors to predict human immunodeficiency virus neutralization efficiency. Cell Host Microbe. 2013;14(5):547–58. https://doi.org/10.1016/j.chom.2013.10.006 PMID: 24237700

15. Herschhorn A, Gu C, Moraca F, Ma X, Farrell M, Smith AB 3rd, et al. The β20-β21 of gp120 is a regulatory switch for HIV-1 Env conformational transitions. Nat Commun. 2017;8(1):1049. Epub 2017/10/19. https://doi.org/10.1038/s41467-017-01119-w PMID: 29051495; PMCID: PMCPMC5648922

16. Herschhorn A, Ma X, Gu C, Ventura JD, Castillo-Menendez L, Melillo B, et al. Release of gp120 restraints leads to an entry-competent intermediate state of the HIV-1 envelope glycoproteins. mBio. 2016;7(5):e01598-16. Epub 2016/10/25. https://doi.org/10.1128/mBio.01598-16 PMID: 27795397; PMCID: PMCPMC5080382

17. Munro JB, Gorman J, Ma X, Zhou Z, Arthos J, Burton DR, et al. Conformational dynamics of single HIV-1 envelope trimers on the surface of native virions. Science. 2014;346(6210):759–63. Epub 2014/10/10. https://doi.org/10.1126/science.1254426 PMID: 25298114; PMCID: PMC4304640

18. Dam K-MA, Fan C, Yang Z, Bjorkman PJ. Intermediate conformations of CD4-bound HIV-1 Env heterotrimers. Nature. 2023;623(7989):1017–25. Epub 20231122. https://doi.org/10.1038/s41586-023-06639-8 PMID: 37993719; PMCID: PMCPMC10686819

19. Li W, Qin Z, Nand E, Grunst MW, Grover JR, Bess JW Jr, et al. HIV-1 Env trimers asymmetrically engage CD4 receptors in membranes. Nature. 2023;623(7989):1026–33. Epub 2023/11/22. https://doi.org/10.1038/s41586-023-06762-6 PMID: 37993716; PMCID: PMCPMC10686830

20. Wang Q, Finzi A, Sodroski J. The conformational states of the HIV-1 envelope glycoproteins. Trends Microbiol. 2020;28(8):655–67. Epub 2020/05/14. https://doi.org/10.1016/j.tim.2020.03.007 PMID: 32418859; PMCID: PMCPMC7363548

21. Colin P, Ringe RP, Yasmeen A, Ozorowski G, Ketas TJ, Lee W-H, et al. Conformational antigenic heterogeneity as a cause of the persistent fraction in HIV-1 neutralization. Retrovirology. 2023;20(1):9. Epub 2023/05/27. https://doi.org/10.1186/s12977-023-00624-9 PMID: 37244989; PMCID: PMCPMC10221750

22. Kwong PD, Doyle ML, Casper DJ, Cicala C, Leavitt SA, Majeed S, et al. HIV-1 evades antibody-mediated neutralization through conformational masking of receptor-binding sites. Nature. 2002;420(6916):678–82. Epub 2002/12/13. https://doi.org/10.1038/nature01188 PMID: 12478295

23. Richman DD, Wrin T, Little SJ, Petropoulos CJ. Rapid evolution of the neutralizing antibody response to HIV type 1 infection. Proc Natl Acad Sci U S A. 2003;100(7):4144–9. Epub 2003/03/20. https://doi.org/10.1073/pnas.0630530100 PMID: 12644702; PMCID: PMC153062

24. Wei X, Decker JM, Wang S, Hui H, Kappes JC, Wu X, et al. Antibody neutralization and escape by HIV-1. Nature. 2003;422(6929):307–12. Epub 2003/03/21. https://doi.org/10.1038/nature01470 PMID: 12646921

25. Ivan B, Sun Z, Subbaraman H, Friedrich N, Trkola A. CD4 occupancy triggers sequential pre-fusion conformational states of the HIV-1 envelope trimer with relevance for broadly neutralizing anti-body activity. PLoS Biol. 2019;17(1):e3000114. Epub 2019/01/16. https://doi.org/10.1371/journal.pbio.3000114 PMID: 30650070; PMCID: PMCPMC6351000

26. Han Q, Jones JA, Nicely NI, Reed RK, Shen X, Mansouri K, et al. Difficult-to-neutralize global HIV-1 isolates are neutralized by antibodies targeting open envelope conformations. Nat Commun. 2019;10(1):2898. Epub 20190701. https://doi.org/10.1038/s41467-019-10899-2 PMID: 31263112; PMCID: PMCPMC6602974

27. Lee M, Lu M, Zhang B, Zhou T, Katte R, Han Y, et al. HIV-1-envelope trimer transitions from prefusion-closed to CD4-bound-open conformations through an occluded-intermediate state. bioRxiv. 2024. Epub 20240717. https://doi.org/10.1101/2024.07.15.603531 PMID: 39071380; PMCID: PMCPMC11275901

28. Parthasarathy D, Pothula KR, Ratnapriya S, Cervera Benet H, Parsons R, Huang X, et al. Conforma-tional flexibility of HIV-1 envelope glycoproteins modulates transmitted/founder sensitivity to broadly neutralizing antibodies. Nat Commun. 2024;15(1):7334. Epub 20240826. https://doi.org/10.1038/s41467-024-51656-4 PMID: 39187497; PMCID: PMCPMC11347675

29. Wang H, Barnes CO, Yang Z, Nussenzweig MC, Bjorkman PJ. Partially open HIV-1 envelope struc-tures exhibit conformational changes relevant for coreceptor binding and fusion. Cell Host Microbe. 2018;24(4):579–592.e4. https://doi.org/10.1016/j.chom.2018.09.003 PMID: 30308160; PMCID: PMCPMC6185872

30. Wang S, Chan K-W, Wei D, Ma X, Liu S, Hu G, et al. Human CD4-binding site antibody elicited by polyvalent DNA prime-protein boost vaccine neutralizes cross-clade tier-2-HIV strains. Nat Commun. 2024;15(1):4301. Epub 2024/05/21. https://doi.org/10.1038/s41467-024-48514-8 PMID: 38773089; PMCID: PMCPMC11109196.

31. Yang Z, Dam K-MA, Gershoni JM, Zolla-Pazner S, Bjorkman PJ. Antibody recognition of CD4-induced open HIV-1 Env trimers. J Virol. 2022;96(24):e0108222. Epub 2022/11/30. https://doi.org/10.1128/jvi.01082-22 PMID: 36448805; PMCID: PMCPMC9769388

32. Beauparlant D, Rusert P, Magnus C, Kadelka C, Weber J, Uhr T, et al. Delineating CD4 depen-dency of HIV-1: adaptation to infect low level CD4 expressing target cells widens cellular tropism but severely impacts on envelope functionality. PLoS Pathog. 2017;13(3):e1006255. Epub 20170306. https://doi.org/10.1371/journal.ppat.1006255 PMID: 28264054; PMCID: PMCPMC5354460

33. Chakrabarti BK, Walker LM, Guenaga JF, Ghobbeh A, Poignard P, Burton DR, et al. Direct antibody access to the HIV-1 membrane-proximal external region positively correlates with neutralization sensitivity. J Virol. 2011;85(16):8217–26. Epub 2011/06/10. https://doi.org/10.1128/JVI.00756-11 PMID: 21653673; PMCID: PMC3147955

34. Haim H, Strack B, Kassa A, Madani N, Wang L, Courter JR, et al. Contribution of intrinsic reactivity of the HIV-1 envelope glycoproteins to CD4-independent infection and global inhibitor sensitivity. PLoS Pathog. 2011;7(6):e1002101. Epub 2011/07/07. https://doi.org/10.1371/journal.ppat.1002101 PMID: 21731494; PMCID: PMC3121797

35. O'Connell O, Repik A, Reeves JD, Gonzalez-Perez MP, Quitadamo B, Anton ED, et al. Efficiency of bridging-sheet recruitment explains HIV-1 R5 envelope glycoprotein sensitivity to soluble CD4 and macrophage tropism. J Virol. 2013;87(1):187–98. Epub 20121010. https://doi.org/10.1128/JVI.01834-12 PMID: 23055568; PMCID: PMCPMC3536387

36. Seaman MS, Janes H, Hawkins N, Grandpre LE, Devoy C, Giri A, et al. Tiered categorization of a diverse panel of HIV-1 Env pseudoviruses for assessment of neutralizing antibodies. J Virol. 2010;84(3):1439–52. Epub 2009/11/27. https://doi.org/10.1128/JVI.02108-09 PMID: 19939925; PMCID: PMC2812321

37. Huang J, Ofek G, Laub L, Louder MK, Doria-Rose NA, Longo NS, et al. Broad and potent neutralization of HIV-1 by a gp41-specific human antibody. Nature. 2012;491(7424):406–12. Epub 2012/11/16. https://doi.org/10.1038/nature11544 PMID: 23151583

38. Walker LM, Huber M, Doores KJ, Falkowska E, Pejchal R, Julien J-P, et al. Broad neutralization coverage of HIV by multiple highly potent antibodies. Nature. 2011;477(7365):466–70. Epub 2011/08/19. https://doi.org/10.1038/nature10373 PMID: 21849977; PMCID: PMC3393110

39. Wu X, Yang Z-Y, Li Y, Hogerkorp C-M, Schief WR, Seaman MS, et al. Rational design of envelope identifies broadly neutralizing human monoclonal antibodies to HIV-1. Science. 2010;329(5993):856–61. Epub 2010/07/10. https://doi.org/10.1126/science.1187659 PMID: 20616233; PMCID: PMC2965066

40. Chuang G-Y, Acharya P, Schmidt SD, Yang Y, Louder MK, Zhou T, et al. Residue-level prediction of HIV-1 antibody epitopes based on neutralization of diverse viral strains. J Virol. 2013;87(18):10047–58. Epub 2013/07/12. https://doi.org/10.1128/JVI.00984-13 PMID: 23843642; PMCID: PMC3753990

41. Georgiev IS, Doria-Rose NA, Zhou T, Kwon YD, Staupe RP, Moquin S, et al. Delineating antibody recognition in polyclonal sera from patterns of HIV-1 isolate neutralization. Science. 2013;340(6133):751–6. Epub 2013/05/11. https://doi.org/10.1126/science.1233989 PMID: 23661761

42. deCamp A, Hraber P, Bailer RT, Seaman MS, Ochsenbauer C, Kappes J, et al. Global panel of HIV-1 Env reference strains for standardized assessments of vaccine-elicited neutralizing antibodies. J Virol. 2014;88(5):2489–507. Epub 2013/12/20. https://doi.org/10.1128/JVI.02853-13 PMID: 24352443; PMCID: PMC3958090

43. Doria-Rose NA, Altae-Tran HR, Roark RS, Schmidt SD, Sutton MS, Louder MK, et al. Mapping polyclonal HIV-1 antibody responses via next-generation neutralization fingerprinting. PLoS Pathog. 2017;13(1):e1006148. Epub 20170104. https://doi.org/10.1371/journal.ppat.1006148 PMID: 28052137; PMCID: PMCPMC5241146

44. Parker Miller E, Finkelstein MT, Erdman MC, Seth PC, Fera D. A structural update of neutralizing epitopes on the HIV envelope, a moving target. Viruses. 2021;13(9):1774. Epub 20210905. https://doi.org/10.3390/v13091774 PMID: 34578355; PMCID: PMCPMC8472920

45. Sanders RW, Derking R, Cupo A, Julien J-P, Yasmeen A, de Val N, et al. A next-generation cleaved, soluble HIV-1 Env trimer, BG505 SOSIP.664 gp140, expresses multiple epitopes for broadly neutralizing but not non-neutralizing antibodies. PLoS Pathog. 2013;9(9):e1003618. Epub 2013/09/27. https://doi.org/10.1371/journal.ppat.1003618 PMID: 24068931; PMCID: PMC3777863

46. Guzzo C, Zhang P, Liu Q, Kwon AL, Uddin F, Wells AI, et al. Structural constraints at the trimer apex stabilize the HIV-1 envelope in a closed, antibody-protected conformation. mBio. 2018;9(6):e00955-18. Epub 2018/12/11. https://doi.org/10.1128/mBio.00955-18 PMID: 30538178; PMCID: PMCPMC6299476

47. Powell RLR, Totrov M, Itri V, Liu X, Fox A, Zolla-Pazner S. Plasticity and epitope exposure of the HIV-1 envelope trimer. J Virol. 2017;91(17):e00410-17. https://doi.org/10.1128/JVI.00410-17 PMID: 28615206

48. Yoon H, Macke J, West AP Jr, Foley B, Bjorkman PJ, Korber B, et al. CATNAP: a tool to compile, analyze and tally neutralizing antibody panels. Nucleic Acids Res. 2015;43(W1):W213-9. Epub 2015/06/04. https://doi.org/10.1093/nar/gkv404 PMID: 26044712; PMCID: PMCPMC4489231

49. Kadelka C, Liechti T, Ebner H, Schanz M, Rusert P, Friedrich N, et al. Distinct, IgG1-driven antibody response landscapes demarcate individuals with broadly HIV-1 neutralizing activity. J Exp Med. 2018;215(6):1589–608. Epub 2018/05/24. https://doi.org/10.1084/jem.20180246 PMID: 29794117

50. Williams KL, Cortez V, Dingens AS, Gach JS, Rainwater S, Weis JF, et al. HIV-specific CD4-induced antibodies mediate broad and potent antibody-dependent cellular cytotoxicity activity and are commonly detected in plasma from HIV-infected humans. EBioMedicine. 2015;2(10):1464–77. https://doi.org/10.1016/j.ebiom.2015.09.001 PMID: 26629541; PMCID: PMCPMC4634620

51. Friedrich N, Stiegeler E, Glögl M, Lemmin T, Hansen S, Kadelka C, et al. Distinct conformations of the HIV-1 V3 loop crown are targetable for broad neutralization. Nat Commun. 2021;12(1):6705. Epub 2021/11/18. https://doi.org/10.1038/s41467-021-27075-0 PMID: 34795280; PMCID: PMCPMC8602657

52. Powell RLR, Totrov M, Itri V, Liu X, Fox A, Zolla-Pazner S. Plasticity and epitope exposure of the HIV-1 envelope trimer. J Virol. 2017;91(17):e00410-17. Epub 2017/08/10. https://doi.org/10.1128/JVI.00410-17 PMID: 28615206; PMCID: PMCPMC5553165

53. Pantophlet R, Ollmann Saphire E, Poignard P, Parren PWHI, Wilson IA, Burton DR. Fine mapping of the interaction of neutralizing and nonneutralizing monoclonal antibodies with the CD4 binding site of human immunodeficiency virus type 1 gp120. J Virol. 2003;77(1):642–58. Epub 2002/12/13. https://doi.org/10.1128/jvi.77.1.642-658.2003 PMID: 12477867; PMCID: PMC140633

54. Walker LM, Phogat SK, Chan-Hui P-Y, Wagner D, Phung P, Goss JL, et al. Broad and potent neutralizing antibodies from an African donor reveal a new HIV-1 vaccine target. Science. 2009;326(5950):285–9. Epub 2009/09/05. https://doi.org/10.1126/science.1178746 PMID: 19729618

55. Ruprecht CR, Krarup A, Reynell L, Mann AM, Brandenberg OF, Berlinger L, et al. MPER-specific antibodies induce gp120 shedding and irreversibly neutralize HIV-1. J Exp Med. 2011;208(3):439–54. Epub 20110228. https://doi.org/10.1084/jem.20101907 PMID: 21357743; PMCID: PMCPMC3058584

56. Julien J-P, Cupo A, Sok D, Stanfield RL, Lyumkis D, Deller MC, et al. Crystal structure of a soluble cleaved HIV-1 envelope trimer. Science. 2013;342(6165):1477–83. Epub 2013/11/02. https://doi.org/10.1126/science.1245625 PMID: 24179159

57. Stewart-Jones GBE, Soto C, Lemmin T, Chuang G-Y, Druz A, Kong R, et al. Trimeric HIV-1-Env structures define glycan shields from clades A, B, and G. Cell. 2016;165(4):813–26. Epub 2016/04/27. https://doi.org/10.1016/j.cell.2016.04.010 PMID: 27114034

58. Calarese DA, Scanlan CN, Zwick MB, Deechongkit S, Mimura Y, Kunert R, et al. Antibody domain exchange is an immunological solution to carbohydrate cluster recognition. Science. 2003;300(5628):2065–71. Epub 2003/06/28. https://doi.org/10.1126/science.1083182 PMID: 12829775

59. Kong L, Lee JH, Doores KJ, Murin CD, Julien J-P, McBride R, et al. Supersite of immune vulnerability on the glycosylated face of HIV-1 envelope glycoprotein gp120. Nat Struct Mol Biol. 2013;20(7):796–803. Epub 2013/05/28. https://doi.org/10.1038/nsmb.2594 PMID: 23708606; PMCID: PMC3823233

60. Lee JH, Andrabi R, Su C-Y, Yasmeen A, Julien J-P, Kong L, et al. A broadly neutralizing antibody targets the dynamic HIV envelope trimer apex via a long, rigidified, and anionic β-hairpin structure. Immunity. 2017;46(4):690–702. https://doi.org/10.1016/j.immuni.2017.03.017 PMID: 28423342; PMCID: PMCPMC5400778

61. Garces F, Sok D, Kong L, McBride R, Kim HJ, Saye-Francisco KF, et al. Structural evolution of glycan recognition by a family of potent HIV antibodies. Cell. 2014;159(1):69–79. https://doi.org/10.1016/j.cell.2014.09.009 PMID: 25259921; PMCID: PMCPMC4278586

62. Sok D, Pauthner M, Briney B, Lee JH, Saye-Francisco KL, Hsueh J, et al. A prominent site of antibody vulnerability on HIV envelope incorporates a motif associated with CCR5 binding and its camouflaging glycans. Immunity. 2016;45(1):31–45. https://doi.org/10.1016/j.immuni.2016.06.026 PMID: 27438765; PMCID: PMCPMC4990068

63. Kwong PD, Wyatt R, Robinson J, Sweet RW, Sodroski J, Hendrickson WA. Structure of an HIV gp120 envelope glycoprotein in complex with the CD4 receptor and a neutralizing human antibody. Nature. 1998;393(6686):648–59. Epub 1998/06/26. https://doi.org/10.1038/31405 PMID: 9641677

64. Liu J, Bartesaghi A, Borgnia MJ, Sapiro G, Subramaniam S. Molecular architecture of native HIV-1 gp120 trimers. Nature. 2008;455(7209):109–13. Epub 2008/08/01. https://doi.org/10.1038/nature07159 PMID: 18668044; PMCID: PMC2610422

65. Rizzuto CD, Wyatt R, Hernández-Ramos N, Sun Y, Kwong PD, Hendrickson WA, et al. A conserved HIV gp120 glycoprotein structure involved in chemokine receptor binding. Science. 1998;280(5371):1949–53. Epub 1998/06/25. https://doi.org/10.1126/science.280.5371.1949 PMID: 9632396

66. Sullivan N, Sun Y, Sattentau Q, Thali M, Wu D, Denisova G, et al. CD4-Induced conformational changes in the human immunodeficiency virus type 1 gp120 glycoprotein: consequences for virus entry and neutralization. J Virol. 1998;72(6):4694–703. Epub 1998/05/30. https://doi.org/10.1128/JVI.72.6.4694-4703.1998 PMID: 9573233; PMCID: PMC109994

67. Trkola A, Dragic T, Arthos J, Binley JM, Olson WC, Allaway GP, et al. CD4-dependent, antibody-sensitive interactions between HIV-1 and its co-receptor CCR-5. Nature. 1996;384(6605):184–7. Epub 1996/11/14. https://doi.org/10.1038/384184a0 PMID: 8906796

68. Glögl M, Friedrich N, Cerutti G, Lemmin T, Kwon YD, Gorman J, et al. Trapping the HIV-1 V3 loop in a helical conformation enables broad neutralization. Nat Struct Mol Biol. 2023;30(9):1323–36. Epub 2023/08/21. https://doi.org/10.1038/s41594-023-01062-z PMID: 37605043; PMCID: PMCPMC10497408

69. Crispin M, Ward AB, Wilson IA. Structure and immune recognition of the HIV glycan shield. Annu Rev Biophys. 2018;47:499–523. Epub 20180329. https://doi.org/10.1146/annurev-biophys-060414-034156 PMID: 29595997; PMCID: PMCPMC6163090

70. Berndsen ZT, Chakraborty S, Wang X, Cottrell CA, Torres JL, Diedrich JK, et al. Visualization of the HIV-1 Env glycan shield across scales. Proc Natl Acad Sci U S A. 2020;117(45):28014–25. Epub 2020/10/22. https://doi.org/10.1073/pnas.2000260117 PMID: 33093196; PMCID: PMCPMC7668054

71. Kong L, Wilson IA, Kwong PD. Crystal structure of a fully glycosylated HIV-1 gp120 core reveals a stabilizing role for the glycan at Asn262. Proteins. 2015;83(3):590–6. https://doi.org/10.1002/prot.24747 PMID: 25546301

72. Crooks ET, Tong T, Chakrabarti B, Narayan K, Georgiev IS, Menis S, et al. Vaccine-elicited tier 2 HIV-1 neutralizing antibodies bind to quaternary epitopes involving glycan-deficient patches proximal

to the CD4 binding site. PLoS Pathog. 2015;11(5):e1004932. Epub 2015/05/30. https://doi.org/10.1371/journal.ppat.1004932 PMID: 26023780; PMCID: PMC4449185

73. Kolchinsky P, Mirzabekov T, Farzan M, Kiprilov E, Cayabyab M, Mooney LJ, et al. Adaptation of a CCR5-using, primary human immunodeficiency virus type 1 isolate for CD4-independent replication. J Virol. 1999;73(10):8120–6. Epub 1999/09/11. https://doi.org/10.1128/JVI.73.10.8120-8126.1999 PMID: 10482561; PMCID: PMC112828

74. Xiang S-H, Finzi A, Pacheco B, Alexander K, Yuan W, Rizzuto C, et al. A V3 loop-dependent gp120 element disrupted by CD4 binding stabilizes the human immunodeficiency virus envelope glycoprotein trimer. J Virol. 2010;84(7):3147–61. Epub 2010/01/22. https://doi.org/10.1128/JVI.02587-09 PMID: 20089638; PMCID: PMC2838131

75. Pancera M, Zhou T, Druz A, Georgiev IS, Soto C, Gorman J, et al. Structure and immune recognition of trimeric pre-fusion HIV-1 Env. Nature. 2014;514(7523):455–61. Epub 2014/10/09. https://doi.org/10.1038/nature13808 PMID: 25296255; PMCID: PMC4348022

76. Polonis VR, Brown BK, Rosa Borges A, Zolla-Pazner S, Dimitrov DS, Zhang M-Y, et al. Recent advances in the characterization of HIV-1 neutralization assays for standardized evaluation of the antibody response to infection and vaccination. Virology. 2008;375(2):315–20. Epub 20080325. https://doi.org/10.1016/j.virol.2008.02.007 PMID: 18367229

77. Brown BK, Wieczorek L, Sanders-Buell E, Rosa Borges A, Robb ML, Birx DL, et al. Cross-clade neutralization patterns among HIV-1 strains from the six major clades of the pandemic evaluated and compared in two different models. Virology. 2008;375(2):529–38. Epub 20080422. https://doi.org/10.1016/j.virol.2008.02.022 PMID: 18433824

78. Cohen YZ, Lorenzi JCC, Seaman MS, Nogueira L, Schoofs T, Krassnig L, et al. Neutralizing activity of broadly neutralizing anti-HIV-1 antibodies against clade B clinical isolates produced in peripheral blood mononuclear cells. J Virol. 2018;92(5):e01883-17. Epub 20180212. https://doi.org/10.1128/JVI.01883-17 PMID: 29237833; PMCID: PMCPMC5809738

79. Mann AM, Rusert P, Berlinger L, Kuster H, Günthard HF, Trkola A. HIV sensitivity to neutralization is determined by target and virus producer cell properties. AIDS. 2009;23(13):1659–67. https://doi.org/10.1097/QAD.0b013e32832e9408 PMID: 19581791

80. Polonis VR, Schuitemaker H, Bunnik EM, Brown BK, Scarlatti G. Impact of host cell variation on the neutralization of HIV-1 in vitro. Curr Opin HIV AIDS. 2009;4(5):400–7. https://doi.org/10.1097/COH.0b013e32832edc50 PMID: 20048704

81. Rusert P, Mann A, Huber M, von Wyl V, Gunthard HF, Trkola A. Divergent effects of cell environment on HIV entry inhibitor activity. AIDS. 2009;23(11):1319–27. Epub 2009/07/07. https://doi.org/10.1097/qad.0b013e32832d92c2 PMID: 19579289

82. Cimbro R, Gallant TR, Dolan MA, Guzzo C, Zhang P, Lin Y, et al. Tyrosine sulfation in the second variable loop (V2) of HIV-1 gp120 stabilizes V2-V3 interaction and modulates neutralization sensitivity. Proc Natl Acad Sci U S A. 2014;111(8):3152–7. https://doi.org/10.1073/pnas.1314718111 PMID: 24569807

83. Lorenzi JCC, Mendoza P, Cohen YZ, Nogueira L, Lavine C, Sapiente J, et al. Neutralizing activity of broadly neutralizing anti-HIV-1 antibodies against primary African isolates. J Virol. 2021;95(5):e01909-20. Epub 2020/12/09. https://doi.org/10.1128/JVI.01909-20 PMID: 33298542; PMCID: PMCPMC8092834

84. Dingens AS, Haddox HK, Overbaugh J, Bloom JD. Comprehensive mapping of HIV-1 escape from a broadly neutralizing antibody. Cell Host Microbe. 2017;21(6):777–787.e4. https://doi.org/10.1016/j.chom.2017.05.003 PMID: 28579254

85. Verbist BMP, Thys K, Reumers J, Wetzels Y, Van der Borght K, Talloen W, et al. VirVarSeq: a low-frequency virus variant detection pipeline for Illumina sequencing using adaptive base-calling accuracy filtering. Bioinformatics. 2015;31(1):94–101. Epub 20140831. https://doi.org/10.1093/bioinformatics/btu587 PMID: 25178459

86. Hodge EA, Chatterjee A, Chen C, Naika GS, Laohajaratsang M, Mangala Prasad V, et al. An HIV-1 broadly neutralizing antibody overcomes structural and dynamic variation through highly focused epitope targeting. Npj Viruses. 2023;1(1):2. Epub 2023/10/05. https://doi.org/10.1038/s44298-023-00002-4 PMID: 38665238; PMCID: PMCPMC11041648

87. Jaworski JP, Cahn P. Preventive and therapeutic features of broadly neutralising monoclonal antibodies against HIV-1. Lancet HIV. 2018;5(12):e723–31. Epub 20180921. https://doi.org/10.1016/S2352-3018(18)30174-7 PMID: 30245003

88. Bradley T, Trama A, Tumba N, Gray E, Lu X, Madani N, et al. Amino acid changes in the HIV-1 gp41 membrane proximal region control virus neutralization sensitivity. EBioMedicine. 2016;12:196–207. Epub 20160831. https://doi.org/10.1016/j.ebiom.2016.08.045 PMID: 27612593; PMCID: PMCPMC5078591

89. O'Rourke SM, Schweighardt B, Phung P, Mesa KA, Vollrath AL, Tatsuno GP, et al. Sequences in glycoprotein gp41, the CD4 binding site, and the V2 domain regulate sensitivity and resistance of HIV-1 to broadly neutralizing antibodies. J Virol. 2012;86(22):12105–14. Epub 20120829. https://doi.org/10.1128/JVI.01352-12 PMID: 22933284; PMCID: PMCPMC3486483

90. Pacheco B, Alsahafi N, Debbeche O, Prévost J, Ding S, Chapleau J-P, et al. Residues in the gp41 ectodomain regulate HIV-1 envelope glycoprotein conformational transitions induced by gp120-directed inhibitors. J Virol. 2017;91(5):e02219-16. Epub 20170214. https://doi.org/10.1128/JVI.02219-16 PMID: 28003492; PMCID: PMCPMC5309946

91. Ringe R, Bhattacharya J. Association of enhanced HIV-1 neutralization by a single Y681H substitution in gp41 with increased gp120-CD4 interaction and macrophage infectivity. PLoS One. 2012;7(5):e37157. Epub 2012/05/19. https://doi.org/10.1371/journal.pone.0037157 PMID: 22606344; PMCID: PMC3351407

92. Deen KC, McDougal JS, Inacker R, Folena-Wasserman G, Arthos J, Rosenberg J, et al. A soluble form of CD4 (T4) protein inhibits AIDS virus infection. Nature. 1988;331(6151):82–4. Epub 1988/01/07. https://doi.org/10.1038/331082a0 PMID: 3257544

93. Fisher RA, Bertonis JM, Meier W, Johnson VA, Costopoulos DS, Liu T, et al. HIV infection is blocked in vitro by recombinant soluble CD4. Nature. 1988;331(6151):76–8. Epub 1988/01/07. https://doi.org/10.1038/331076a0 PMID: 2829022

94. Allaway GP, Davis-Bruno KL, Beaudry GA, Garcia EB, Wong EL, Ryder AM, et al. Expression and characterization of CD4-IgG2, a novel heterotetramer that neutralizes primary HIV type 1 isolates. AIDS Res Hum Retroviruses. 1995;11(5):533–9. Epub 1995/05/01. https://doi.org/10.1089/aid.1995.11.533 PMID: 7576908

95. Barbas CF 3rd, Björling E, Chiodi F, Dunlop N, Cababa D, Jones TM, et al. Recombinant human Fab fragments neutralize human type 1 immunodeficiency virus in vitro. Proc Natl Acad Sci U S A. 1992;89(19):9339–43. Epub 1992/10/01. https://doi.org/10.1073/pnas.89.19.9339 PMID: 1384050; PMCID: PMC50122

96. Parren PW, Gauduin MC, Koup RA, Poignard P, Fisicaro P, Burton DR, et al. Relevance of the antibody response against human immunodeficiency virus type 1 envelope to vaccine design. Immunol Lett. 1997;57(1–3):105–12. Epub 1997/06/01. https://doi.org/10.1016/s0165-2478(97)00043-6 PMID: 9232434

97. Sok D, van Gils MJ, Pauthner M, Julien J-P, Saye-Francisco KL, Hsueh J, et al. Recombinant HIV envelope trimer selects for quaternary-dependent antibodies targeting the trimer apex. Proc Natl Acad Sci U S A. 2014;111(49):17624–9. Epub 20141124. https://doi.org/10.1073/pnas.1415789111 PMID: 25422458; PMCID: PMCPMC4267403

98. Trkola A, Purtscher M, Muster T, Ballaun C, Buchacher A, Sullivan N, et al. Human monoclonal antibody 2G12 defines a distinctive neutralization epitope on the gp120 glycoprotein of human immunodeficiency virus type 1. J Virol. 1996;70(2):1100–8. Epub 1996/02/01. https://doi.org/10.1128/JVI.70.2.1100-1108.1996 PMID: 8551569; PMCID: PMC189917

99. Muster T, Steindl F, Purtscher M, Trkola A, Klima A, Himmler G, et al. A conserved neutralizing epitope on gp41 of human immunodeficiency virus type 1. J Virol. 1993;67(11):6642–7. Epub 1993/11/01. https://doi.org/10.1128/JVI.67.11.6642-6647.1993 PMID: 7692082; PMCID: PMC238102

100. Stiegler G, Kunert R, Purtscher M, Wolbank S, Voglauer R, Steindl F, et al. A potent cross-clade neutralizing human monoclonal antibody against a novel epitope on gp41 of human immunodeficiency virus type 1. AIDS Res Hum Retroviruses. 2001;17(18):1757–65. Epub 2002/01/15. https://doi.org/10.1089/08892220152741450 PMID: 11788027

101. Zwick MB, Labrijn AF, Wang M, Spenlehauer C, Saphire EO, Binley JM, et al. Broadly neutralizing antibodies targeted to the membrane-proximal external region of human immunodeficiency virus type 1 glycoprotein gp41. J Virol. 2001;75(22):10892–905. Epub 2001/10/17. https://doi.org/10.1128/JVI.75.22.10892-10905.2001 PMID: 11602729; PMCID: PMC114669

102. Buchacher A, Predl R, Strutzenberger K, Steinfellner W, Trkola A, Purtscher M, et al. Generation of human monoclonal antibodies against HIV-1 proteins; electrofusion and Epstein-Barr virus transformation for peripheral blood lymphocyte immortalization. AIDS Res Hum Retroviruses. 1994;10(4):359–69. https://doi.org/10.1089/aid.1994.10.359 PMID: 7520721

103. Scheid JF, Mouquet H, Feldhahn N, Seaman MS, Velinzon K, Pietzsch J, et al. Broad diversity of neutralizing antibodies isolated from memory B cells in HIV-infected individuals. Nature. 2009;458(7238):636–40. Epub 2009/03/17. https://doi.org/10.1038/nature07930 PMID: 19287373

104. Gorny MK, Conley AJ, Karwowska S, Buchbinder A, Xu JY, Emini EA, et al. Neutralization of diverse human immunodeficiency virus type 1 variants by an anti-V3 human monoclonal antibody. J Virol. 1992;66(12):7538–42. Epub 1992/12/01. https://doi.org/10.1128/JVI.66.12.7538-7542.1992 PMID: 1433529; PMCID: PMC240465

105. Scherrer AU, Traytel A, Braun DL, Calmy A, Battegay M, Cavassini M, et al. Cohort profile update: the Swiss HIV cohort study (SHCS). Int J Epidemiol. 2022;51(1):33–34j. https://doi.org/10.1093/ije/dyab141 PMID: 34363666

106. Braun DL, Kouyos RD, Balmer B, Grube C, Weber R, Günthard HF. Frequency and spectrum of unexpected clinical manifestations of primary HIV-1 infection. Clin Infect Dis. 2015;61(6):1013–21. Epub 2015/05/19. https://doi.org/10.1093/cid/civ398 PMID: 25991469

107. Rusert P, Fischer M, Joos B, Leemann C, Kuster H, Flepp M, et al. Quantification of infectious HIV-1 plasma viral load using a boosted in vitro infection protocol. Virology. 2004;326(1):113–29. https://doi.org/10.1016/j.virol.2004.05.022 PMID: 15262500

108. Wu X, Parast AB, Richardson BA, Nduati R, John-Stewart G, Mbori-Ngacha D, et al. Neutralization escape variants of human immunodeficiency virus type 1 are transmitted from mother to infant. J Virol. 2006;80(2):835–44. https://doi.org/10.1128/JVI.80.2.835-844.2006 PMID: 16378985

109. Koyanagi Y, Miles S, Mitsuyasu RT, Merrill JE, Vinters HV, Chen IS. Dual infection of the central nervous system by AIDS viruses with distinct cellular tropisms. Science. 1987;236(4803):819–22. https://doi.org/10.1126/science.3646751 PMID: 3646751

110. Hess JF, Kohl TA, Kotrová M, Rönsch K, Paprotka T, Mohr V, et al. Library preparation for next generation sequencing: a review of automation strategies. Biotechnol Adv. 2020;41:107537. Epub 2020/03/19. https://doi.org/10.1016/j.biotechadv.2020.107537 PMID: 32199980

111. Nelson MC, Morrison HG, Benjamino J, Grim SL, Graf J. Analysis, optimization and verification of illumina-generated 16S rRNA gene amplicon surveys. PLoS One. 2014;9(4):e94249. Epub 2014/04/10. https://doi.org/10.1371/journal.pone.0094249 PMID: 24722003; PMCID: PMCPMC3983156

112. Brandenberg OF, Magnus C, Rusert P, Regoes RR, Trkola A. Different infectivity of HIV-1 strains is linked to number of envelope trimers required for entry. PLoS Pathog. 2015;11(1):e1004595. Epub 20150108. https://doi.org/10.1371/journal.ppat.1004595 PMID: 25569556; PMCID: PMCPMC4287578

113. Li H, et al. Seqtk: a fast and lightweight tool for processing FASTA or FASTQ sequences; 2023. Available from: https://github.com/lh3/seqtk

114. Wickham H. ggplot2: elegant graphics for data analysis. New York, NY: Springer; 2009. p. VIII, 213.

115. Galili T, O'Callaghan A, Sidi J, Sievert C. heatmaply: an R package for creating interactive cluster heatmaps for online publishing. Bioinformatics. 2018;34(9):1600–2. https://doi.org/10.1093/bioinformatics/btx657 PMID: 29069305

116. Wickham H, Averick M, Bryan J, Chang W, McGowan L, François R, et al. Welcome to the Tidyverse. J Open Source Softw. 2019;4(43):1686. https://doi.org/10.21105/joss.01686

117. Harrell FE. Hmisc: a package of miscellaneous R function; 2023. Available from: https://hbiostat.org/R/Hmisc/